

LEVEL

12

SC5202.11FR

15

Copy No. _____

SC5202.11FR

ADA1022272

GROWTH OF HgCdTe BY MODIFIED MOLECULAR BEAM EPITAXY

FINAL TECHNICAL REPORT FOR PHASE I
February 12, 1979 through February 11, 1981

CONTRACT NO. MDA903-79-C-0188
DARPA Order No. 3704

Prepared for

Defense Advanced Research Projects Agency
1400 Wilson Boulevard
Arlington, VA 22209

J. T. Cheung
Principal Investigator
(805) 498-4545, x-144



JUNE 1981

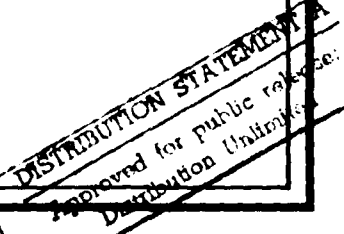
This research was sponsored by the Defense Advanced Research Projects under DARPA Order No. 3704, Contract No.: MDA903-79-C-0188; Monitored by Defense Supply Service.

The views and conclusions contained in this document are those of the author and should not be interpreted as necessarily representing the official policies, either expressed or implied, of the Defense Advanced Research Projects Agency or the United States Government.

Effective Date of Contract: 02/12/79
Contract Expiration Date: 02/11/81



Rockwell International
Science Center



81 7 31 093

UNCLASSIFIED(9) Final rept. 12 Feb 79-11
Feb 81 on Phase 1,

SECURITY CLASSIFICATION OF THIS PAGE (When Data Entered)

REPORT DOCUMENTATION PAGE			READ INSTRUCTIONS BEFORE COMPLETING FORM
1. REPORT NUMBER	2. GOVT ACCESSION NO.	3. RECIPIENT'S CATALOG NUMBER	
AD-A102272			
4. TITLE (AND SUBTITLE) GROWTH OF HgCdTe BY MODIFIED MOLECULAR BEAM EPITAXY		5. TYPE OF REPORT & PERIOD COVERED Final Report-Phase I 02/12/79 through 02/11/81	
6. AUTHOR(s) J. T. Cheung		7. PERFORMING ORGANIZATION NAME AND ADDRESS Rockwell International Science Center 1049 Camino Dos Rios Thousand Oaks, CA 91360	
8. CONTROLLING OFFICE NAME AND ADDRESS Defense Advanced Research Projects Agency 1400 Wilson Blvd. Arlington, VA 22209		9. REPORT DATE June 81	
10. MONITORING AGENCY NAME & ADDRESS (if different from Controlling Office)		11. NUMBER OF PAGES 70	
(12) 72		12. SECURITY CLASS. (of this report) Unclassified	
		13a. DECLASSIFICATION/DOWNGRADING SCHEDULE	
14. DISTRIBUTION STATEMENT (of this Report) Approved for public release; distribution unlimited.			
15. DISTRIBUTION STATEMENT (of the abstract entered in Block 20, if different from Report)			
16. SUPPLEMENTARY NOTES			
17. KEY WORDS (Continue on reverse side if necessary and identify by block number) Thin film, HgCdTe, laser evaporation			
18. ABSTRACT (Continue on reverse side if necessary and identify by block number) A novel technique for depositing thin film has been developed. In this technique, a pulsed laser is used as an external power source for evaporation. The laser can also provide in situ beam processing capability when the beam is directed onto the substrate surface. Using this technique, we have demonstrated that Hg_xCd_{1-x}Te films can be prepared by laser evaporating a HgTe/CdTe mixture. When the deposition takes place in a high vacuum, the film is Hg deficient. However, when it is carried (over)			

UNCLASSIFIED

SECURITY CLASSIFICATION OF THIS PAGE (When Data Entered)

1000222

out in a Hg back-pressure as low as 2×10^{-5} Torr, the film becomes stoichiometric. Various alloy compositions can be obtained by adjusting the ratio of HgTe and CdTe in the source mixture.

UNCLASSIFIED

SECURITY CLASSIFICATION OF THIS PAGE (When Data Entered)

TABLE OF CONTENTS

	<u>Page</u>
1.0 OBJECTIVES.....	1
2.0 EXPERIMENTAL.....	5
2.1 Apparatus Description.....	7
2.2 Film Characterization.....	10
3.0 RESULTS.....	11
3.1 Interaction of High Power Laser Radiation with Solid Surface.....	11
3.2 Evaporation Mechanism.....	16
3.2.1 Evaporation Under High Power Density.....	18
3.2.2 Evaporation Under Intermediate Power Density.....	20
3.2.3 Evaporation Under Low Power Density.....	26
3.3 Deposition Mechanism and Film Properties.....	41
3.3.1 Deposition Under High Laser Power Density.....	43
3.3.2 Deposition Under Intermediate Power Density.....	44
3.3.3 Deposition Under Low Power Density.....	48
4.0 CONCLUSION.....	60
5.0 FUTURE PLAN.....	63
6.0 REFERENCES.....	65

Accession For
 NTIS GRA&I
 DTIC TAB
 Unannounced
 Justification

By _____
 Distribution/
 Availability Codes
 Avail and/or
 Dist Spec
 Other
 Special

A

LIST OF FIGURES

<u>Figure</u>		<u>Page</u>
1	Scheme of a LADA apparatus.....	6
2	Surface temperature of a source material after pulsed and CW irradiation.....	15
3	Depth dependence of peak temperature.....	17
4	Surface of a thin film deposited by using very high power laser pulse.....	19
5	Mass spectrum of evaporating $Hg_{0.7}Cd_{0.3}Te$ using intermediate power laser pulses.....	21
6	Time-of-flight spectrum of Hg evaporated from $Hg_{0.7}Cd_{0.3}Te$ by laser pulse.....	23
7	Angular dependence of the splashed particles.....	24
8	Angular dependence of the film thicknesses.....	25
9	Mass spectrum of laser evaporated HgTe.....	27
10	Evaporation rate of Hg from HgTe as a function of the scanning rate.....	29
11	Surface temperature evolution due to overlapping laser pulses.....	30
12	Mass spectrum of laser evaporated CdTe.....	32
13	Evaporation rate of Cd from CdTe as a function of the scanning rate.....	33
14	Variation of Cd to Te from CdTe under various laser irradiating conditions.....	37
15	Mass spectrum of laser evaporate HgTe/CdTe mixture.....	39
16	Evaporate rate of Hg and Cd from a HgTe/CdTe mixture as a function of the scanning rate.....	40
17	Mass spectrum of laser evaporated bulk $Hg_{0.7}Cd_{0.3}Te$ material....	42
18	IR transmission spectrum of a HgCdTe film.....	45

LIST OF FIGURES

<u>Figure</u>		<u>Page</u>
19	Spectral response of a HgCdTe photoconductor.....	47
20	IR transmission spectra of HgCdTe films deposited under different vacuum conditions.....	51
21a	Surface of a HgCdTe film.....	53
21b	Cross section view of a HgCdTe film.....	54
22	Rutherford backscattering of 3700 Å $Hg_{0.7}Cd_{0.3}Te$ on CdTe.....	55
23	Surface of a HgCdTe film deposited at 170°C.....	57
24	$Hg_{0.7}Cd_{0.3}Te$ film on CdTe after thermal treatment.....	58

ACKNOWLEDGMENTS

The work reported in this document was performed at the Rockwell International Science Center, Thousand Oaks, California, with the support of the Defense Advanced Research Project Agency under contract No. MDA903-79-C-0188.

Dr. D.T. Cheung is the Program Manager and Dr. J.T. Cheung is the Principle Investigator. Support by R.A. Reynolds and S. Roosild are gratefully acknowledged.

V
C3239A/bw

1.0 OBJECTIVES

In recent years, HgCdTe has become one of the most important infrared detector materials. Of the many growth techniques that exist for this material, epitaxial growth on CdTe substrates appears to be the best approach. It not only produces films with quality better than those grown by the bulk growth technique, but its geometrical structure also is more suitable for fabricating focal plane arrays. The backbone of this technique is liquid phase epitaxy (LPE). Although high performance detectors have been realized with LPE, there still are areas that need improvement; these include:

1. Large Epilayer Size. Growing large epilayers can reduce the material and processing cost.
2. Growth on Foreign Substrates. While CdTe is an ideal substrate material for HgCdTe, the size of a single crystal CdTe substrate is limited ($< 25 \text{ cm}^2$). There is currently no existing technique to grow large (>2 in.) diameter single crystal CdTe boules. With this constraint, it is logical to extend the epitaxial growth technique to allow the growth of HgCdTe thin films on more commonly available substrates, e.g., silicon and germanium. If successful, this approach may by-pass the need for large size CdTe technology. It may also open up new possibilities for infrared focal plane array structures and architectures.

3. Low Growth Temperature. This has always been a major objective for modifying the existing growth techniques or developing a new technique. Low growth temperature means less thermal strain in the resultant film. Low growth temperature also means a reduction of both interdiffusion between the epilayer and the substrate and diffusion of impurities from the substrate material into the epilayer. This problem is especially severe for the HgCdTe/CdTe system. In LPE growth, the temperature is fixed as determined by the solid-liquid equilibria.

4. Multilayer Growth Capability. Many devices have multilayered structures. It is always desirable to be able to form such structures during growth. However, because of the geometrical arrangement and the growth condition, this adaption to some LPE systems is difficult.

Considering these requirements, the vacuum deposition technique seems to be a viable approach. The growth is controlled by kinetics, therefore lower epitaxy temperature is expected. Because it is a deposition process, there is practically no limit to the film size. Multisources can be installed easily for layered-growth. However, because of the volatile nature of HgCdTe, vacuum deposition of this material is not straightforward. Difficulties inherent to this technique are:

1. Evaporation of HgCdTe is non-congruent. Heating of the target can result in a preferential loss of Hg.¹
2. The deposited film starts to lose Hg into the vacuum at temperatures as low as 100°C.

These obstacles suggest that a conventional deposition process is not suitable.

The earliest work on vacuum deposition of HgCdTe was by Ludeke and Paul.² They prepared $Hg_{1-x}Cd_xTe$ film by flash evaporation and obtained film of the same composition as the source material ($x = 0.11$ and $x = 0.48$) at 300 and 450K. Ignatowicz et al³ used the classical vacuum deposition technique to prepare $Hg_{1-x}Cd_xTe$ films ($0.001 < x < 0.25$) from polycrystalline sources ($0.13 < x < 0.88$) at 160°C. The films were Hg deficient. Hohnke et al⁴ have deposited $Hg_xCd_{1-x}Te$ films by flash evaporation of $Hg_{0.8}Cd_{0.2}Te$ and by evaporation of HgTe and CdTe placed in separate Knudsen cells. In both cases, films deposited at an approximate temperature of 100°C were very low in mercury. The loss of mercury was compensated for by adding a mercury source. This technique enabled $Hg_{0.8}Cd_{0.2}Te$ films to be obtained at temperatures up to about 150°C. Above that temperature, the film formed two phases: a $Hg_{1-x}Cd_xTe$ ($x > 0.2$) phase and a tellurium phase. Sputtering deposition has also been extensively used. Pioneering work in sputtering was carried out in an Ar atmosphere.⁵ The resultant films showed loss of mercury. Much better results

SC5202.11FR

could be obtained by carrying out the sputtering process in a Hg plasma.^{6,7}
The films are stoichiometric with some oriented crystallinity.

During the course of this program, we have developed a new thin film deposition technique and have successfully demonstrated that it is capable of producing stoichiometric $Hg_{1-x}Cd_xTe$ films. The x value can be adjusted easily. This technique is quite different from any of the processes mentioned above. It is cleaner and very versatile, and does not require a high energy plasma as in the sputtering process. The experimental approach, the progress, and the results are discussed in the following sections.

2.0 EXPERIMENTAL

The new thin film deposition technique is appropriately named LADA (Laser Assisted Deposition and Annealing), because it uses a high power laser as an external energy source to vaporize source materials as well as to anneal the as deposited films.

The scheme of a LADA apparatus is shown in Fig. 1. A train of laser pulses is directed into the vacuum system and then focused onto the target source. The maximum power density can be as high as a few times 10^8 W/cm² for a duration of several hundred nanoseconds. Each pulse is absorbed by a small volume of source material, causing very rapid heating and cooling. The peak temperature can well exceed the temperature needed for evaporation. Under this extreme condition, material evaporates congruently. The approach is similar to the conventional flash evaporation, but is much cleaner and responds faster because the bulky feeding mechanism and the high temperature strip are replaced by scanning laser pulses. These two methods also have different evaporation mechanisms. The mechanisms for laser evaporating HgTe, CdTe, HgTe/CdTe mixture, and Hg_{0.7}Cd_{0.3}Te bulk crystals were studied by mass spectroscopy; their results will be discussed in Section 3.2.

In the LADA process, the same laser beam can be focused and scanned over the substrate area. If the beam is scanned over the substrate prior to deposition, it can be used to clean the substrate. If the beam is scanned over the substrate during or after deposition, it can do beam

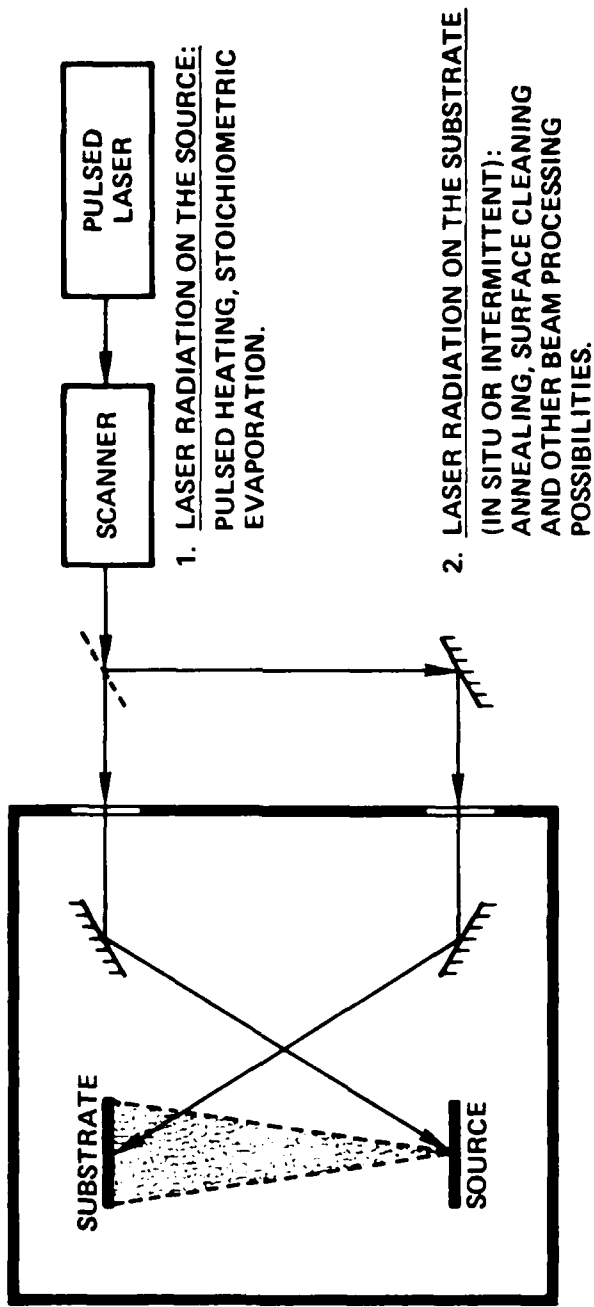


Fig. 1 Scheme of a LADA apparatus.

processing on the as-deposited film. This option adds a new dimension to the system, which we have not yet explored in any depth.

2.1 Apparatus Description

The apparatus consists of two parts, the vacuum chamber and the laser unit.

Main Vacuum Chamber

The main vacuum chamber is 12 inches in diameter and 10 inches tall, and is all metal construction. The vacuum is backed up by two parallel pumping systems, a mercury diffusion pump stack and an ion pump. The mercury diffusion pump was chosen because of its simplicity and low cost; more important, the pump fluid in this case is just mercury, which is one of the component of the $Hg_{1-x}Cd_xTe$ system, and therefore does not create a contamination problem. (Incidentally, mercury diffusion pumps were used in most of the previous sputtering work.) The ion pump was used only for routine system bake out. All the depositions were made by using only the mercury pump. Typical base pressure was 5×10^{-7} torr or lower.

The main chamber has many ports for different accessories, e.g., windows and mirrors for the laser beam, a UTI model 100C mass analyzer for monitoring the evaporation process. One of the vacuum port is connected to a pool of mercury isolated by a valve. By opening this valve and adjusting the

gate valve to the diffusion pump, Hg background pressure can be varied from 2×10^{-5} torr to 10^{-3} torr.

Laser Unit and Optics

We used a Nd-YAG laser (Control Laser Inc. Model 258) with an output wavelength of 1.06 μm . The laser has an acousto-optical Q-switch. Pulse frequency can be varied from 1 kHz to 75 kHz. In the single mode operation, the maximum average power is 15 W; the limiting apertures can be removed for more output power. The maximum attainable power in a multimode output is 100 W. In all our experiments, single mode beam was used because of its better focusing property and spatial homogeneity. The beam characteristics were measured by a factory-calibrated Ge detector. The peak power can be varied by varying the pulse frequency while maintaining the total power output constant. This feature allows us to optimize the laser power for evaporation, without sacrificing the deposition rate.

The laser beam is first expanded by a 5:1 up-collimator, followed by a galvanometric x-y mirror scanner. It then passes through a focus lens and enters the vacuum chamber.

It is essential that there is no line-of-sight connection between the target surface and the vacuum window. Otherwise, the evaporant can rapidly condense on the window and block the laser beam. First we tried to heat the window, but the performance was not satisfactory. A mirror was later installed inside the vacuum system to reflect the laser beam onto the target

surface. With this setup, condensation occurred on the mirror surface, and the reflectivity was slowly reduced. We were, however, able to sustain deposition for a long time; deposition of thick films (a few μm) is now possible, but the mirror needs cleaning after each run. In the future, we will install a heater to heat the mirror to an elevated temperature during deposition; therefore, the problem of condensation on the mirror will be completely avoided.

The laser beam has a Gaussian distribution. At the focal point, the diameter of the spot measured at the 1/e point is approximately 10^{-2} cm. The power densities given in the text are the average over the pulse duration and the spot area. The power is monitored by the Ge detector outside of the vacuum chamber. Actual power level at the target surface would be lower due to losses through the various optical components.

Substrate Holder

The substrate holder has a total area of 1-1/2 in. \times 1-3/4 in. Substrates are mounted onto the holder surface with Ta foil clips to assure sufficient thermal contact. The substrate can be heated up to 700°C by Mo coils, and the temperature can be regulated within 1°C.

Source Material

For the deposition of HgCdTe films, two type of sources were used. At first, we used bulk HgCdTe crystals for evaporation. Later, we switched to

HgTe and CdTe powder mixtures. The homogenized mixtures were pressed in vacuum into pellets, 1/2 in. in diameter under a pressure of 10 ton/cm². Both sources give films of comparable quality. The homogenized mixture source is more suitable for us, because it is readily available and the composition can be adjusted arbitrarily.

For the study of evaporation mechanisms of HgTe and CdTe, pressed pellets of HgTe (Gallard-Schelesinger, 99.995%) and CdTe (Gallard-Schelesinger, 99.999%) were used.

2.2 Film Characterization

Once the film is grown, one of the most important tasks is to determine its composition. For a thin film deposited on CdTe, the composition can be quickly evaluated by optical transmission measurement. In some cases, EDAX (Energy Dispersive X-ray Analysis) was also used.

The electrical properties were determined by Hall measurements.

3.0 RESULTS

In this section, results are presented in the following order:

Section 3.1 gives a comprehensive description of the interaction of high power laser with condensed matter; numerical results on surface temperature calculations are presented. Section 3.2 presents the results on laser evaporating HgTe, CdTe, HgTe/CdTe mixtures and bulk $Hg_{1-x}Cd_xTe$; mass spectroscopic analysis was used to elucidate the mechanism. Section 3.3 presents the properties of the deposited films, their relationship to the deposition mechanism are discussed.

3.1 Interaction of High Power Laser Radiation with Solid Surface

When a high power laser beam interacts with a solid surface, three regions may be distinguished on the basis of the predominant phenomena:

1. In the low power density regime ($< 10^7 \text{ W/cm}^2$), the substance temperature exceeds its melting temperature and passes over into the liquid state followed by recrystallization.
2. In the intermediate power density regime ($\sim 10^7 \text{ W/cm}^2 - 10^9 \text{ W/cm}^2$), the surface absorbs enough energy that vaporization takes place. The evaporants contain mainly neutral species.

3. In the high power density regime ($>10^9 \text{ W/cm}^2$), the substance passes over into a plasma state, where it is largely ionized.

These three regimes fall into the research categories of laser annealing, laser evaporation, and laser fusion, respectively. Therefore, only the first two types of interaction are relevant to the LADA study.

When laser radiation is absorbed at the surface of a condensed matter, heat is developed near the surface and the surface temperature therefore increases. Simultaneously, heat conduction into the interior takes place, thus increasing the thickness of the heated layer. Because the velocity of heat transport due to conduction decreases with time, there is not an adequate outlet of heat into the interior of the material; hence, the temperature at and near the surface will increase until evaporation begins.

Temperature rise due to laser heating can be calculated by solving the differential equation for heat flow. If we limit ourselves to a single material phase, the following assumptions can be made to simplify the problem:

1. The heat flows in one dimension from the surface to the interior.
2. Neglect the blackbody radiation loss and ignore the latent heat associated with a phase transition.
3. All physical constants are temperature independent.

Under these conditions, the differential equation for heat flow into a piece of material with a boundary at $x = 0$ is:

$$\frac{\partial^2 T(x,t)}{\partial x^2} - \frac{1}{K} \frac{\partial T(x,t)}{\partial t} = - \frac{A(x,t)}{K} \quad (1)$$

where T is the temperature, t the time after the turn-on, k the thermal diffusivity, K the thermal conductivity and A is the radiation power density per unit time. The initial and boundary conditions are:

$$T(x,0) = 0$$

$$T(x,t) \rightarrow 0 \quad \text{as } x \rightarrow \infty \quad . \quad (2)$$

For a step source (such as the turn-on of a CW laser):

$$A(x,t) = 0 \quad \text{for } t < 0$$

$$A(x,t) = (I - R)I_0 e^{-\alpha x} \quad \text{for } t > 0 \quad (3)$$

where R is the reflectivity, I_0 is the power density, and α is the absorption coefficient. The solution of Eq. (1) can then be expressed in terms of the complementary error function (erfc) and its integral (ierfc):

$$\begin{aligned}
 T(x,t) = & (I - R) (2I_0/K)(kt)^{1/2} i \operatorname{erfc} [x/2(kt)^{1/2}] - I_0 e^{\alpha x}/K\alpha \\
 & + (I_0/2K\alpha)e^{\alpha^2 kt - \alpha x} \operatorname{erfc} (kt)^{1/2} \alpha - [k/2(kt)^{1/2}] \\
 & + (I_0/2K\alpha)e^{\alpha^2 kt + \alpha x} \operatorname{erfc} (kt)^{1/2} \alpha + [x/2(kt)^{1/2}] . \quad (4)
 \end{aligned}$$

For pulsed operation, the laser pulse can be approximated by a number of successive steps, and the solution corresponds to the superposition of Eq. (4). Using HgCdTe as an example, $R = 0.3$, $\alpha = 10^{-4} \text{ cm}^{-1}$, $K = 0.1 \text{ W/cm} \cdot \text{K}^\circ$, $k = 0.09 \text{ W cm}^2/\text{s}$. We have calculated the surface temperature evolution for both cw ($6 \times 10^4 \text{ W/cm}^2$) and pulsed ($5 \times 10^7 \text{ W/cm}^2$) radiation. The power density quoted here is typical in our experiments. The 200 ns duration pulse is replaced with a three step approximation. The results are shown in Fig. 2. The pulsed radiation produces very high surface temperature, with rapid heating and cooling rate. Under cw radiation, the temperature increases gradually until thermal equilibrium.

In reality, the peak temperature should be lower due to phase changes, but the shape of the temperature curve should basically be unchanged. Three qualitative features of this curve deserve special attention. First, the heating rate is very fast, on the order of $10^{10} \text{ C}^\circ/\text{s}$. Second, a very high peak temperature can be achieved. Third, due to the low thermal conductivity of HgCdTe, the cooling rate is quite slow.

SC5202.11FR

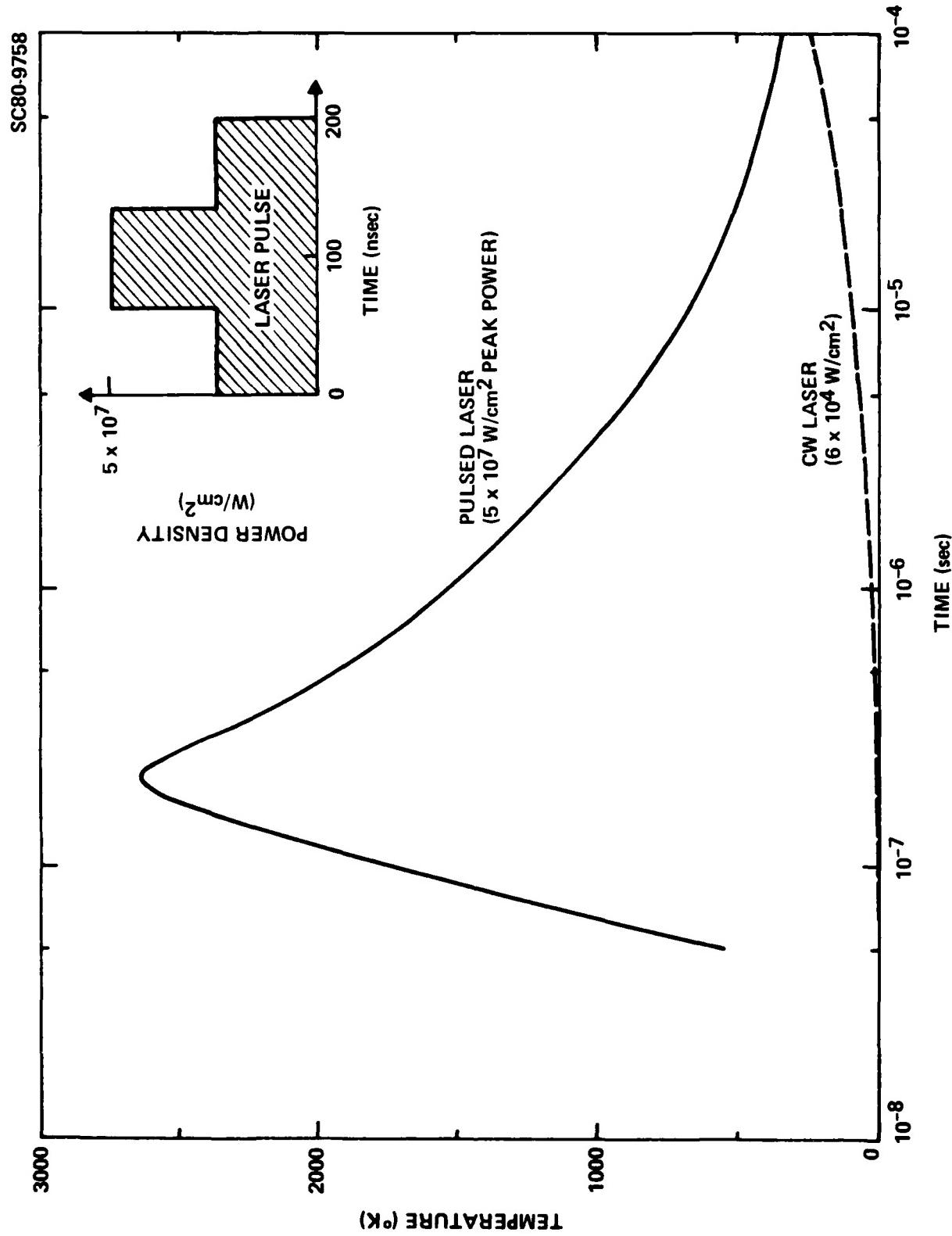


Fig. 2 Surface temperature of a source material after pulsed and CW irradiation.

We have also calculated the temperature evolution curve for different depths. A peak temperature vs depth plot is shown in Fig. 3. Heat penetration can be as deep as 1 μm . The depth can be reduced by lowering the laser power.

3.2 Evaporation Mechanism

The evaporation process depends strongly on two factors: the laser power density and the scanning rate. The laser power density directly affects the surface temperature and the depth of heat penetration; whereas the effects due to scanning rate is indirect and is related to the thermal relaxation of the source material. The materials used for evaporation are HgTe, CdTe, HgTe/CdTe mixture and $\text{Hg}_{1-x}\text{Cd}_x\text{Te}$ bulk crystal. All of them have low thermal conductivity, therefore this effect is significant. The mirror scanner has a frequency range from 0.4 Hz to 100 Hz (over a scanning distance of 1.6 cm), and the laser pulse rate can be varied from 1 kHz to 75 kHz. The combination corresponds to the distance between two consecutive pulses from 10^{-5} cm to almost 0.1 cm. Since the spot size is approximately 10^{-2} cm in diameter, as many as 1000 pulses can overlap the same area at the slowest scanning rate.

Compositional analysis of the evaporant species were made by a quadrupole mass spectrometer; its ionizer was located 4 in. from the source surface and 30° from the incident laser beam. The electron energy in the ionizer was set to be 70 V; this is the same voltage used by Farrows¹ in his study of thermal evaporation of HgCdTe. Therefore, direct comparisons can be made unambiguously.

SC5202.11FR

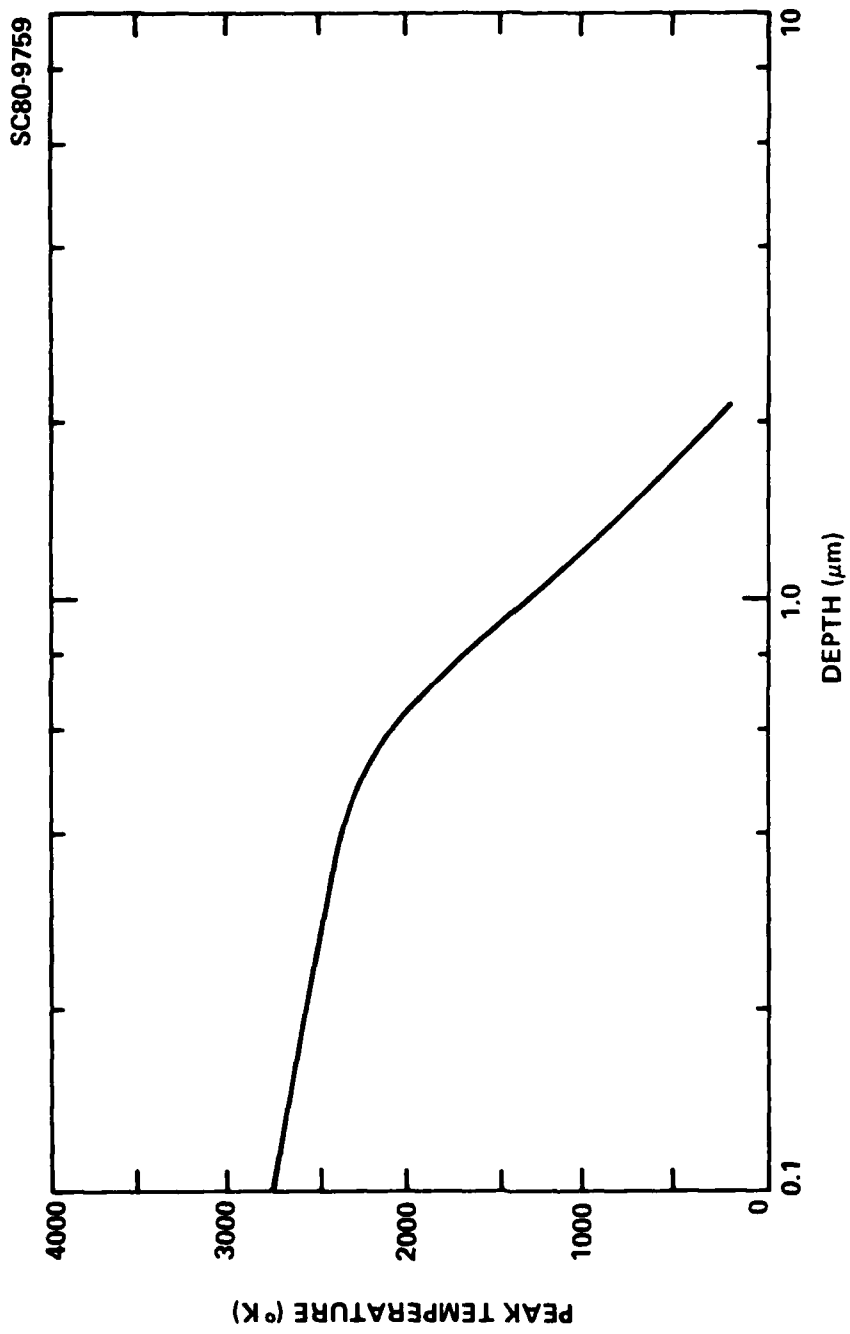


Fig. 3 Depth dependence of peak temperature.

Bulk $Hg_{1-x}Cd_xTe$ was evaporated under three different power density levels, high power ($>10^8 \text{ W/cm}^2$), intermediate power ($\sim 5 \times 10^7 \text{ W/cm}^2$), and low power ($\sim 8 \times 10^6 \text{ W/cm}^2$). Evaporation processes under these conditions vary drastically, with the lowest power level yielding film of the best quality. Therefore the evaporation processes of CdTe, HgTe, and HgTe/CdTe mixture were only studied under the low power level. The following section discusses the evaporation process of each material under various conditions.

3.2.1 Evaporation Under High Power Density

When a piece of bulk $Hg_{0.7}Cd_{0.3}Te$ was placed in the vacuum and irradiated with laser pulses whose power density exceeded 10^8 W/cm^2 , a bright plume was formed over the focal spot. The plume mainly consisted of microparticles which were ejected from the surface at a very high speed. This effect, sometimes referred as "splashing",⁸ occurs when the sub-surface material is heated above its boiling point before the surface material is completely vaporized. Under such condition, the remainder of the top surface material can erupt in the form of small particles. Figure 4 shows the surface morphology of a film deposited under this condition. The surface is covered with a high density of small particles, some of which are irregular solid chuncks and some have the appearance of a condensed molten globule. EDAX measurement indicates that these particles have the same composition as the source material. Films deposited under this condition have rough and inhomogeneous surfaces. Furthermore, the impact of these high velocity particles can induce damage in the as-deposited film; therefore, splashing

SC5202.11FR

SC81-13233

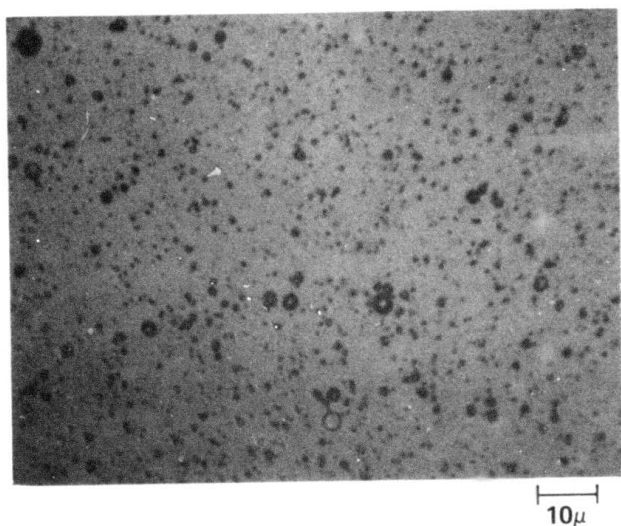


Fig. 4 Surface of a thin film deposited by using very high power laser pulse.

must be avoided. Splashing can be minimized by reducing the laser power level, which in turn reduces the depth of heat penetration.

3.2.2 Evaporation Under Intermediate Power Density

Again, only the bulk $Hg_{0.7}Cd_{0.3}Te$ material was evaporated under this power level ($5 \times 10^7 \text{ W/cm}^2$). Splashing of small particles was no longer a dominant process. The evaporants mainly consisted of atoms and molecular clusters; Fig. 5 shows a mass spectrum of the evaporants. The key observations are:

1. All three atomic species, Hg, Cd, and Te, are present. Their compositional ratio is not the same as the source material. There is an excess of Hg.
2. There is no molecular HgTe, CdTe and Te₂.
3. There is a large abundance of species with mass/charge ratio greater than 360; these can only correspond to clusters such as CdTe₂⁺, Te₃⁺, Hg₂Te₃⁺², etc. Unfortunately, because of the detection limit of the spectrometer, clusters with mass/charge ratio of more than 400 cannot be observed. The spectrum is not corrected for the spectrometer gain, transmission factors, or ionization efficiency; these calibrations are mass and species dependent. Taking these factors into consideration, we conclude

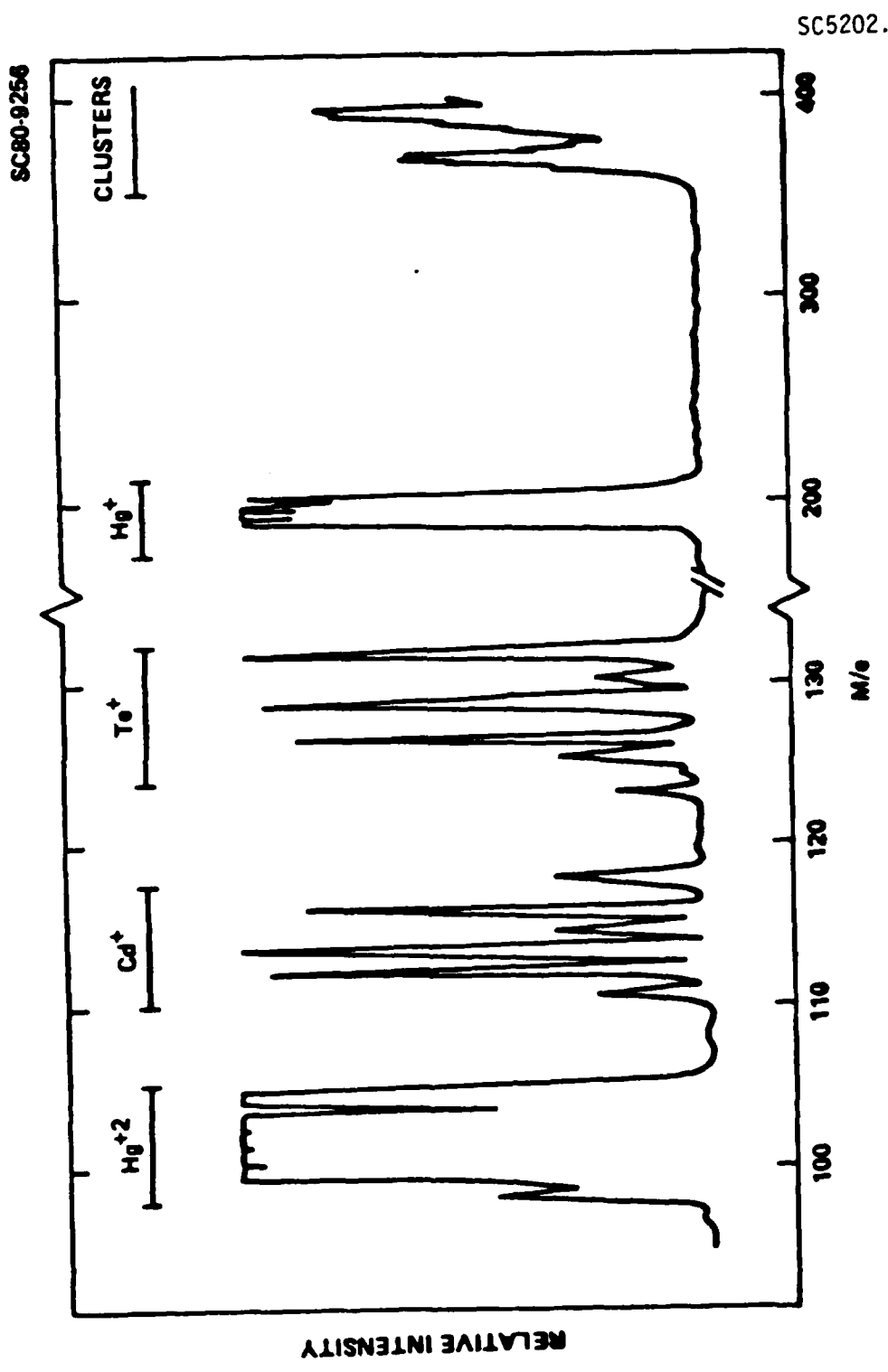


Fig. 5 Mass spectrum of evaporating $\text{Hg}_0.7\text{Cd}_0.3\text{Te}$ using intermediate power laser pulses.

that over 80% of the evaporants (excluding splashed particles) are in the cluster form. The rest are atoms, rich in Hg.

Previous studies showed that the laser evaporated species had very high kinetic energy, typically peaking in the range of a few eV.⁹ The Hg⁺ signal is intense enough for time-of-flight measurement to determine its energy distribution. The experiment is straightforward. A laser pulse was used as the "zero time" reference, and the Hg⁺ signal output was displayed on a storage oscilloscope; the result is shown in Fig. 6. The energy distribution peaks at 5 eV, which is considerably higher than that of a thermal beam. Cd and Te signals were too weak for similar measurement, but it is reasonable to expect them to behave similarly.

Due to the large difference in mass, atoms, clusters and splashed particles will have different angular distributions; this was verified by simple experiment. A number of substrates were placed at equal distance to the evaporation source on a circular holder. After 30 minutes of deposition, films of different thickness and density of the splashed particles were formed. We reason that the smooth area was due to the deposition of clusters, while the micron size particles were due to the condensation of splashing particles. Therefore, the number density of the particles and the film thickness of the smooth area on the various substrates should reflect the angular distribution of the splashed particles and the clusters, respectively. The results are shown in Fig. 7 and Fig. 8. The angular distribution of the splashed particles is narrower. By placing the substrate at a wide

SC5202.11FR

SC80-11226

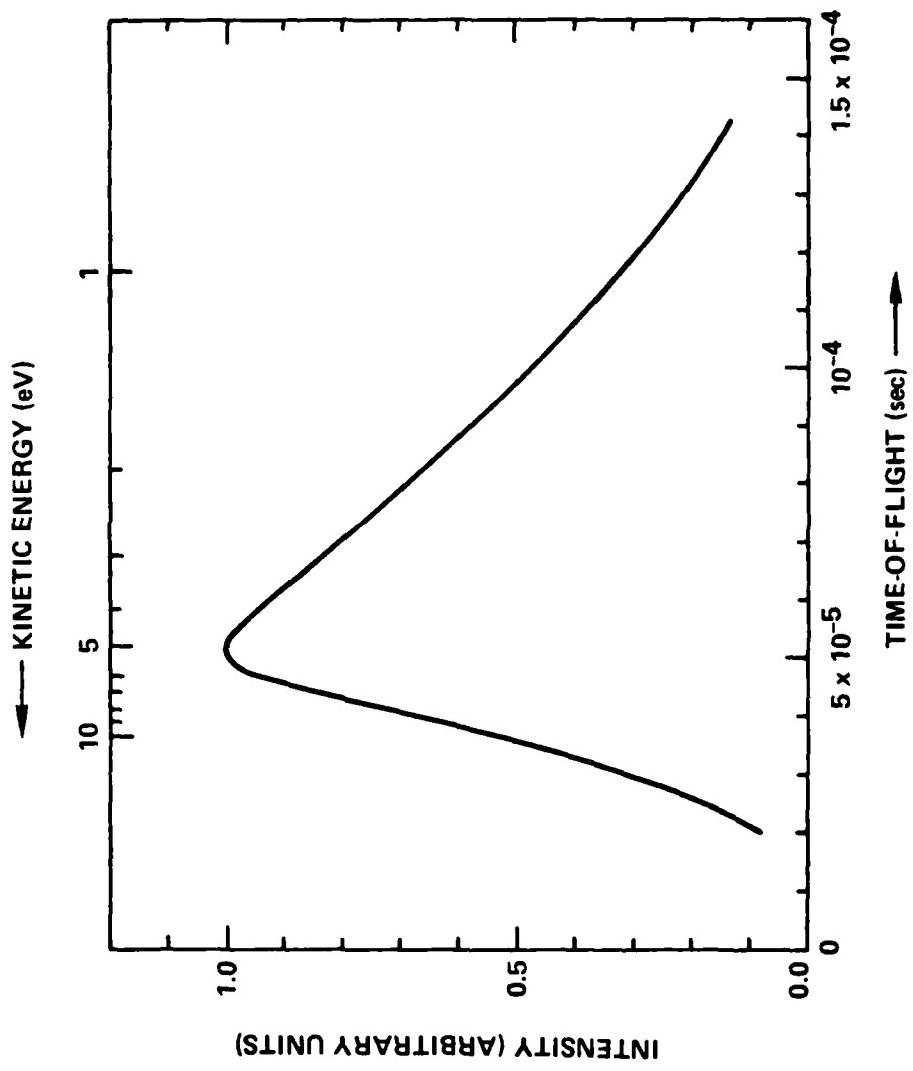


Fig. 6 Time-of-flight spectrum of Hg evaporated from $Hg_0.7Cd_0.3Te$ by laser pulse.

SC5202.11FR

SC80-9255

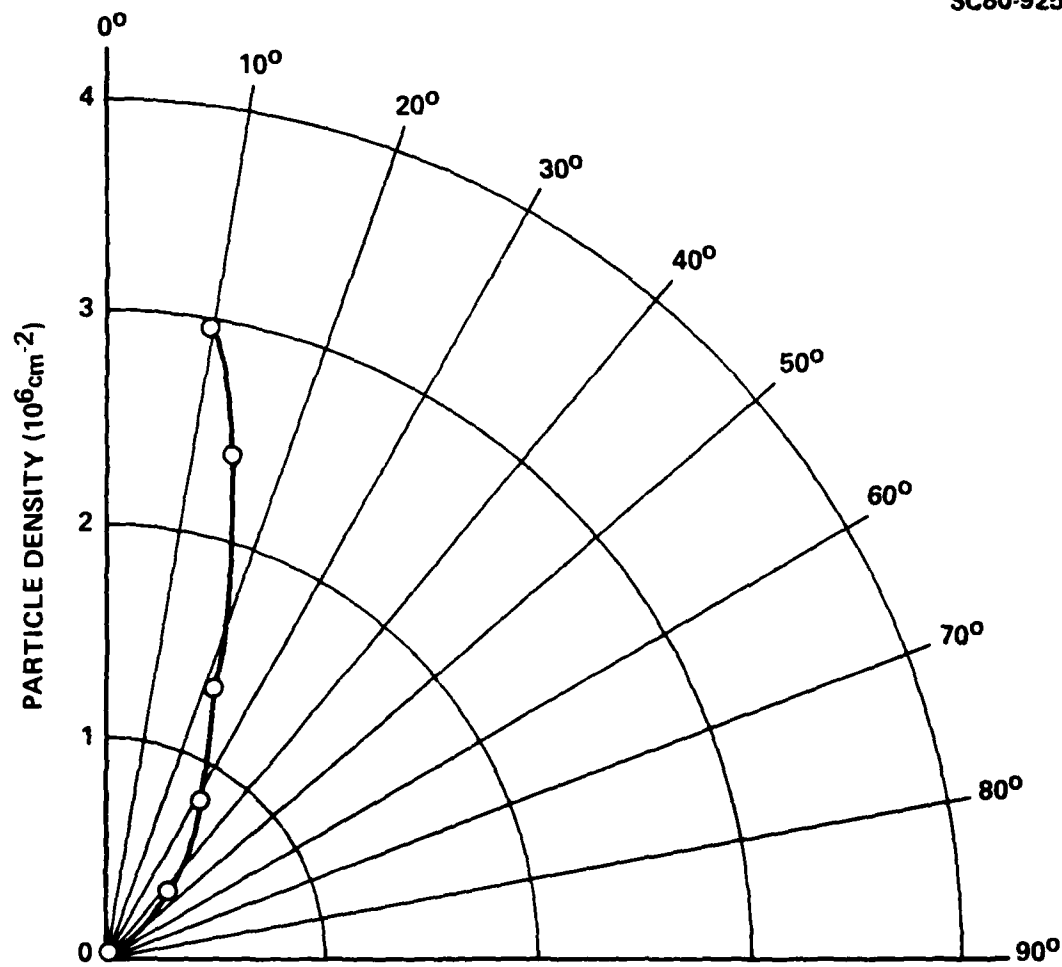


Fig. 7 Angular dependence of the splashed particles.

SC5202.11FR

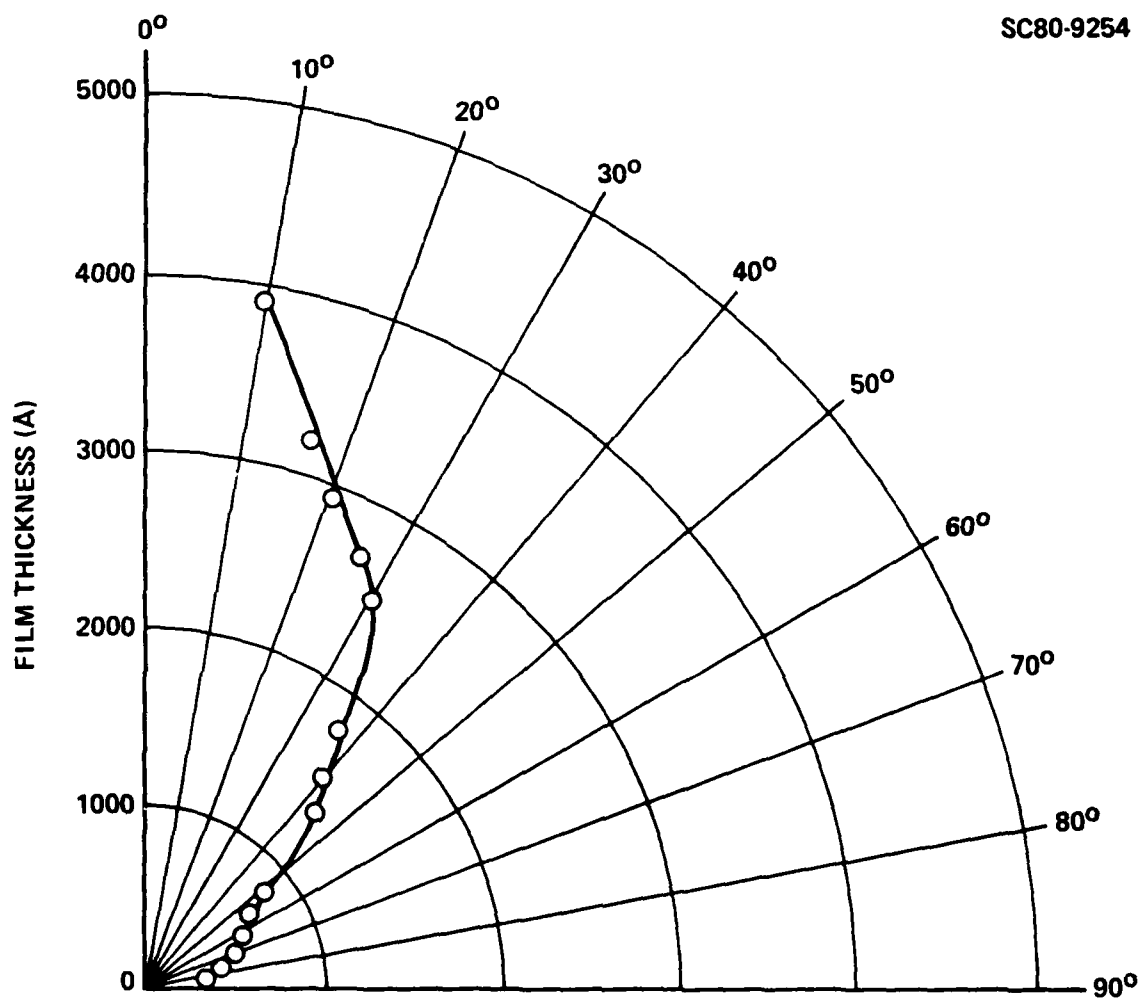


Fig. 8 Angular dependence of the film thicknesses.

angle, one can avoid the splashed particles and intercept the cluster species only. Smooth films can be obtained this way. During the early stage of the program, we used this target - substrate geometry for film deposition.

3.2.3 Evaporation Under Low Power Density

An off axis substrate mounting can reduce the splashing problem, but it also reduces the deposition rate. We therefore tried to minimize the splashing effect by further reducing the laser power. At power density in the neighborhood of 8×10^6 W/cm², the density of the splashed particles becomes very small; the evaporation is still congruent. Results of evaporating HgTe, CdTe, HgTe/CdTe mixture and bulk HgCdTe crystals are discussed in the following sections.

3.2.3.1 Evaporation of HgTe

Hard pressed pellets of HgTe powders (99.995%, G-S Chemical Inc.) were used as source material. The mass spectrum of the evaporants from laser evaporation at a power level of 7×10^6 W/cm² is shown in Fig. 9. The major species are Hg and Te atoms. A trace amount (<1%) of Te₂ molecules is also detectable. The intensity of the different species in the spectrum is not proportional to the actual composition. Corrections should be made on ionization efficiency and a number of other factors. The signal ratio of atomic Hg and Te remains constant through the entire experiment (approximately 1 hr); this is a good indication of a congruent evaporation. If the evaporation is not congruent, as in the thermal case, Hg will be depleted

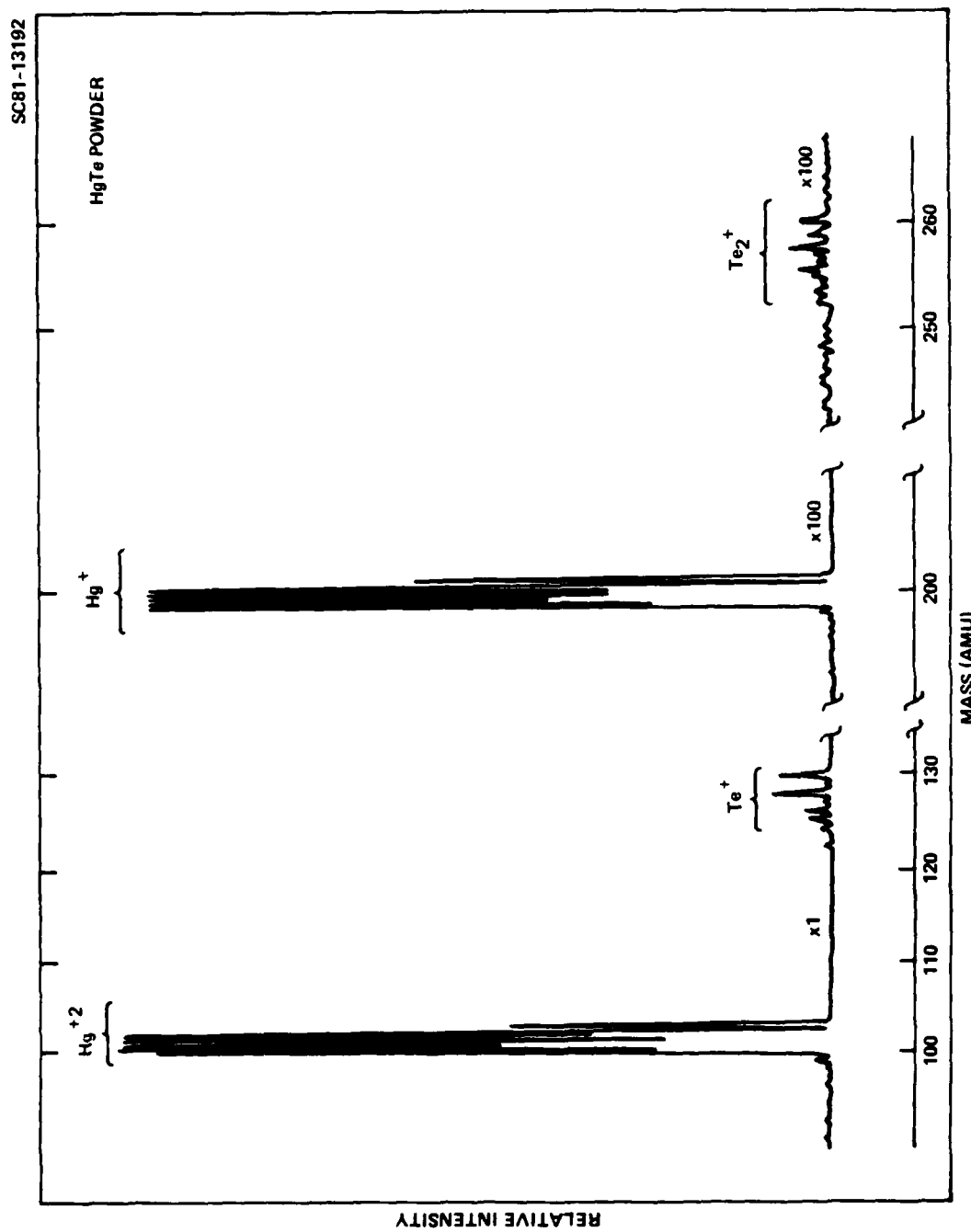


Fig. 9 Mass spectrum of laser evaporated HgTe.

gradually from the surface layer, leaving a tellurium rich skin; this would result in a gradual decrease in the ratio of atomic Hg to Te.

The evaporation rate varies rapidly with the scanning rate. By varying the scanning rate and the laser frequency while keeping the power density per pulse constant, the Hg signal intensity has been plotted as a function of the distance between two consecutive pulses in Fig. 10. The evaporation rate decreases monotonically. The relative ratio of Hg to Te atoms remains constant over the entire range of scanning rate. Only at very slow scanning rate (distance between consecutive pulses $< 10^{-5}$ cm), does the evaporation of Hg atoms increase more rapidly than Te atoms.

This phenomenon is a result of the overlapping of pulses the thermal properties of the material. For example, the spot size of the focused laser beam is approximately 10^{-2} cm diameter; this means that if the pulse-to-pulse distance is 10^{-4} cm, as many as 100 pulses can overlap. For a poor thermal conductor such as HgTe, the nominal time between two pulses (approximately 5×10^{-4} s) is too short for the surface to relax to its original temperature prior to the laser pulse. The surface absorbs more energy from the next pulse while it is still hot and its temperature becomes even higher. This process continues until the last laser pulse moves out of the region. Under this condition, the actual temporal evolution of the surface temperature does not have the form shown in Fig. 2. Instead, it has the form shown in Fig. 11. The surface can be at high temperature for a long time: the slower the scan rate, the longer this duration. Consequently, the evaporation rate increases. However, if the scanning rate is too slow, the heating period may

SC5202.11FR

SC81-13230

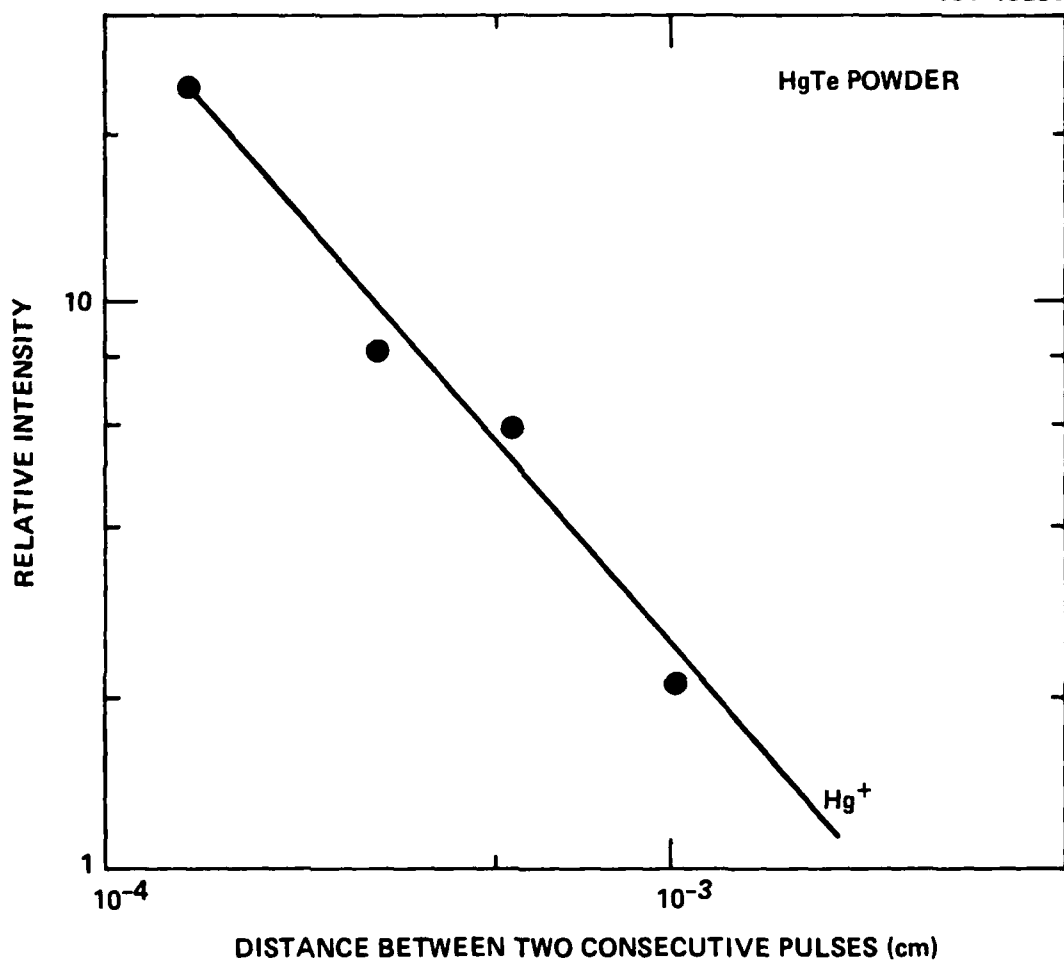
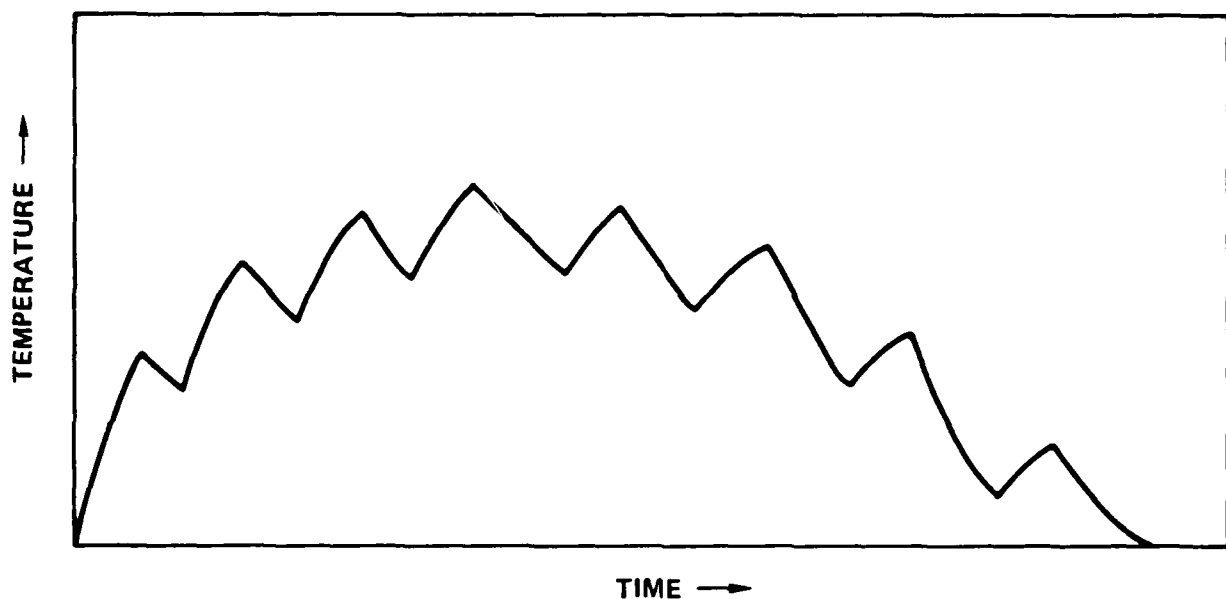


Fig. 10 Evaporation rate of Hg from HgTe as a function of the scanning rate.

SC5202.11FR

SC81-13231



become so long that Hg starts to diffuse to the surface and evaporates preferentially before all the elements leave the surface together. Under this circumstance, the evaporation is similar to the thermal process.¹

3.2.3.2 Evaporation of CdTe

Unlike HgTe, CdTe has a wide band gap and is transparent at the wavelength (1.06 μm) of a Nd-YAG laser; therefore, it is much more difficult to evaporate. We found that laser pulses with power density in the 10^7 W/cm^2 range could not cause any damage to the polished CdTe wafers. Evaporation commenced only when the power level exceeded 10^8 W/cm^2 . For the hard pressed pellet of CdTe powder, the power requirement for evaporation was, however, much less stringent. The interface region between powder particles could absorb the laser radiation effectively, and the heat generated at these interfaces was transferred to the entire volume of the powder particle. The average diameter of the CdTe powders is 2 μm ; the focused spot is 100 μm in diameter, and the absorption depth is approximately 0.5 μm . Therefore, hundreds of such powder interfaces are exposed to each laser pulse.

The mass spectrum of the evaporants is shown in Fig. 12. Atomic Cd and Te are the dominant species, with a trace of Te_2 (< 1%). This is different from the thermal evaporation, where Cd atoms and Te molecules are the only evaporants.¹⁰ The ratio of atomic Cd to Te is constant over the entire range of power level. Just like HgTe, the production rate of Cd from laser evaporating CdTe depends on the scanning rate; the result is shown in Fig. 13. On a logarithmic scale, it has a linear relationship with negative slope, but the

SC5202.11FR

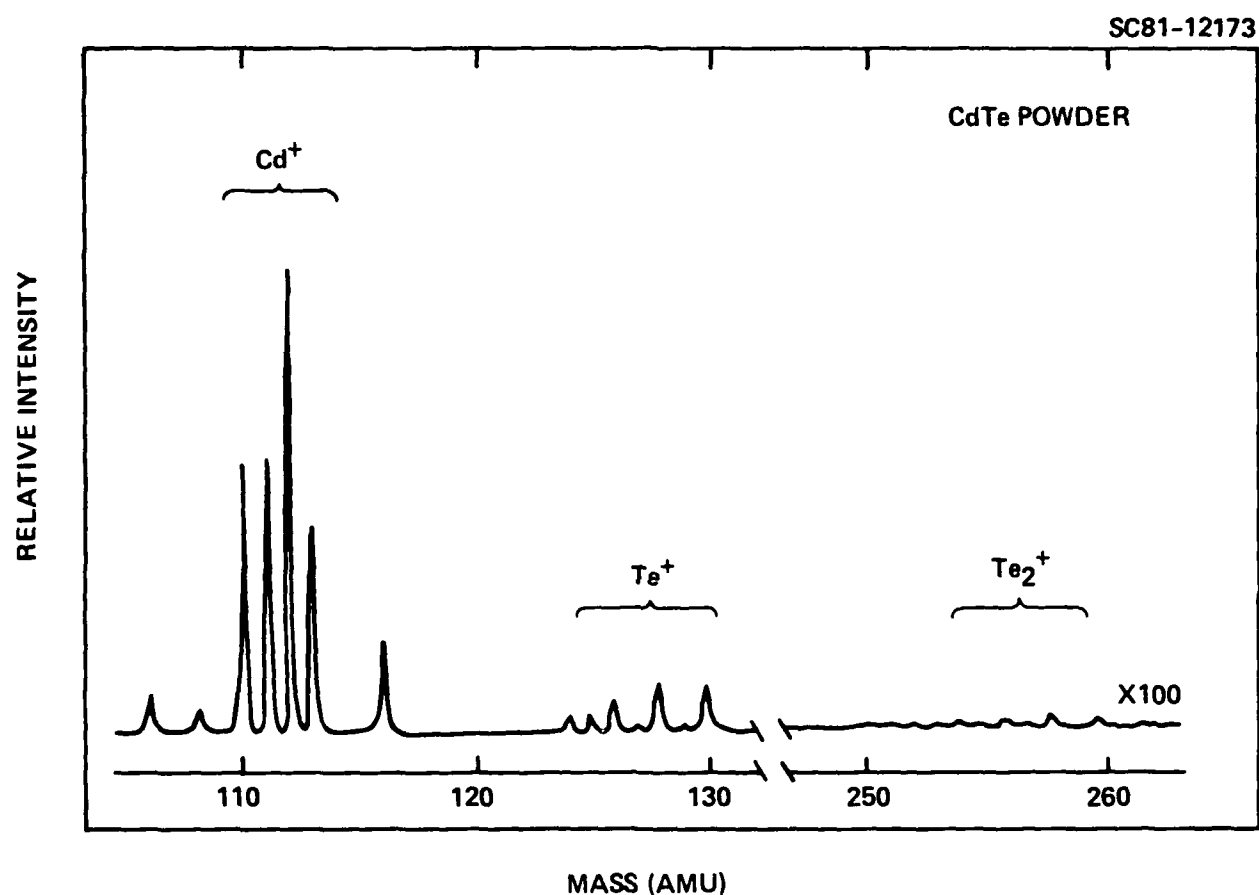


Fig. 12 Mass spectrum of laser evaporated CdTe.

SC5202.11FR

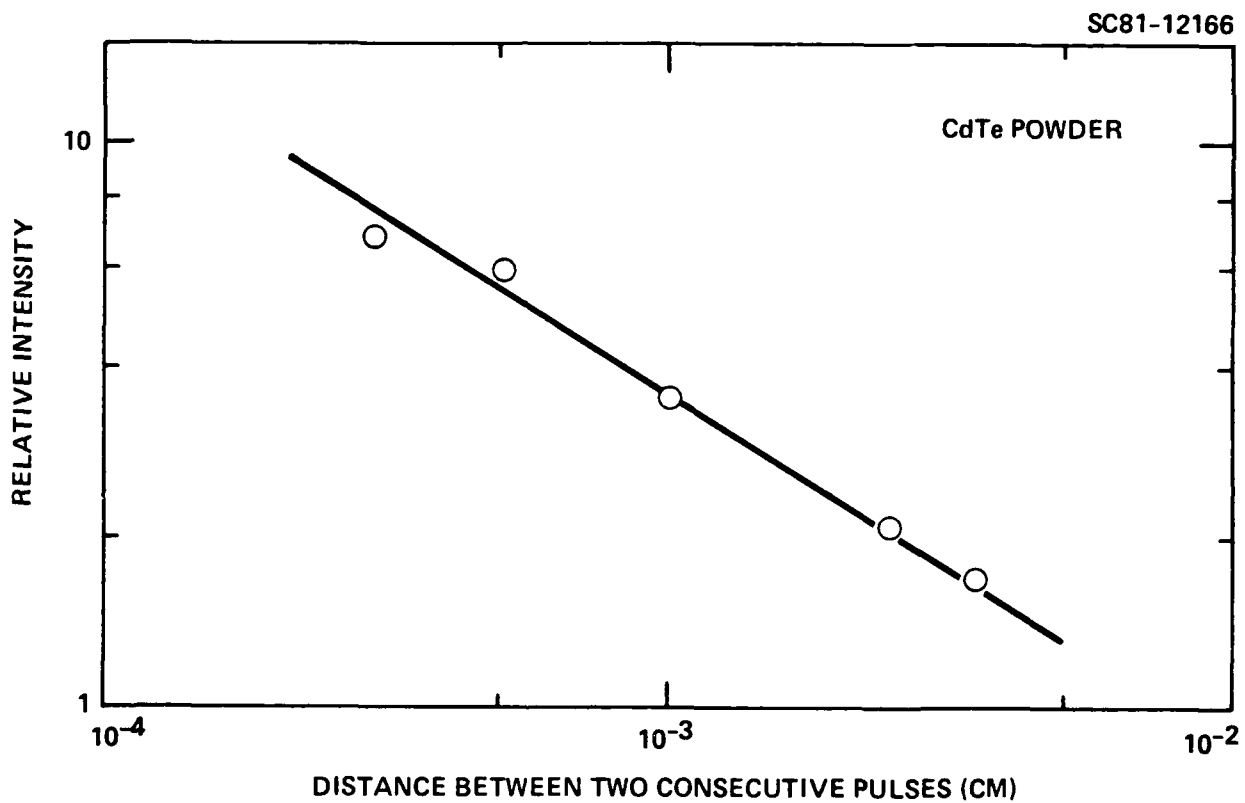


Fig. 13 Evaporation rate of Cd from CdTe as a function of the scanning rate.

33
C3239A/bw

slope is more gradual than that of HgTe. The ratio of atomic Cd to Te remains constant over the entire range of scanning rate.

We have analyzed the chemical composition of a deposited film with XPS (x-ray photoelectron spectroscopy). By comparing it with the standard spectra of a bulk CdTe crystal and thermal evaporated CdTe film we reach the following conclusions:

1. Within the detection sensitivity (< 0.1%), the film is stoichiometric. There is no trace of free cadmium and tellurium. This indicates that the evaporation is congruent, and the cadmium and tellurium atoms from the evaporants recombine to form CdTe molecules on a substrate at room temperature.
2. During the XPS measurement, photoelectrons are ejected from the sample surface under x-ray irradiation. For an insulator, positive charge can build up. A stream of low energy electron is necessary to flood over the irradiated area to maintain surface neutrality. The energy of the electrons needed to compensate this charge build up is a relative measure of the insulating property. For a 2000 Å thick CdTe film deposited by thermal evaporation, the required energy is 1 eV; however, for a laser evaporated CdTe film of the same thickness, more than 12 eV is needed. This suggests that the laser evaporated CdTe film is a better insulator.

Because of the extreme surface condition created by the high power radiation, unusual processes not associated with the conventional thermal evaporation can happen. Some of these unusual evaporation processes of CdTe are worth mentioning, and understanding their occurrence can help optimize the laser evaporation condition.

In one experiment, we compared the difference in evaporation of cw radiation (without scanning) and pulsed radiation (with and without scanning). The average power in all cases was kept constant at 15 W, the energy per pulse was 5 mj, and the scanning was such that the pulse-to-pulse distance was 5×10^{-4} cm. In the case of cw irradiation, a dim spot in the focal point formed almost immediately after the laser was turned on; it reached the brightness of a white glow just a few seconds later. The temperature was measured to be 1700°C with an optical pyrometer. The temperature of the surface under pulse irradiation could not be measured directly because the heating and cooling was too rapid. In all these cases, the mass spectra of the evaporants were very similar; namely, the dominant species were atomic cadmium and tellurium with a trace amount of tellurium molecules. Under pulsed irradiation, the amount of tellurium molecules was less than 1%; under cw irradiation, it increased to almost 3%. The increase of molecular tellerium is consistent with the lower surface temperature and longer duration achieved with the cw irradiation. The most interesting feature is the variation of atomic cadmium to tellurium ratio over a period of time; Fig. 14 shows the Cd to Te ratio measured during the first 1200 seconds under these conditions. Under pulsed irradiation with scanning, the ratio remained constant,

indicating a case of congruent evaporation; under pulsed irradiation without scanning, the ratio decreased gradually with time and reached a constant level after more than 1000 sec. The ratio at zero time, obtained by extrapolation to zero time, agrees with the ratio obtained in the congruent case. Under cw irradiation, the ratio falls more rapidly and approaches to the same constant level only the 250 s later. The zero extrapolation again intercepts the value for congruent evaporation.

This can be interpreted in terms of a preferential vaporization of Cd from the CdTe surface under a prolonged high temperature condition. This condition can be created either by cw laser irradiation or pulsed irradiation without scanning. During this time, more Cd diffuses from the bulk to supplement the loss at the surface, until a steady state is established. The asymptotic Cd to Te ratio in Fig. 14 is indicative of this state. It takes a longer time to reach this state under pulse irradiation (no scanning) than cw irradiation.

The overall picture of preferential evaporation of Cd and Hg from CdTe and HgTe, respectively, is very similar. The only difference is that Cd depletion occurs at a much higher temperature.

3.2.3.3 Evaporation of HgTe/CdTe Mixture

In the latter part of our program, we demonstrated the use of a mixture of HgTe/CdTe powders as a source for depositing HgCdTe films. The evaporation mechanism was studied and compared to that of the two component

SC5202.11FR

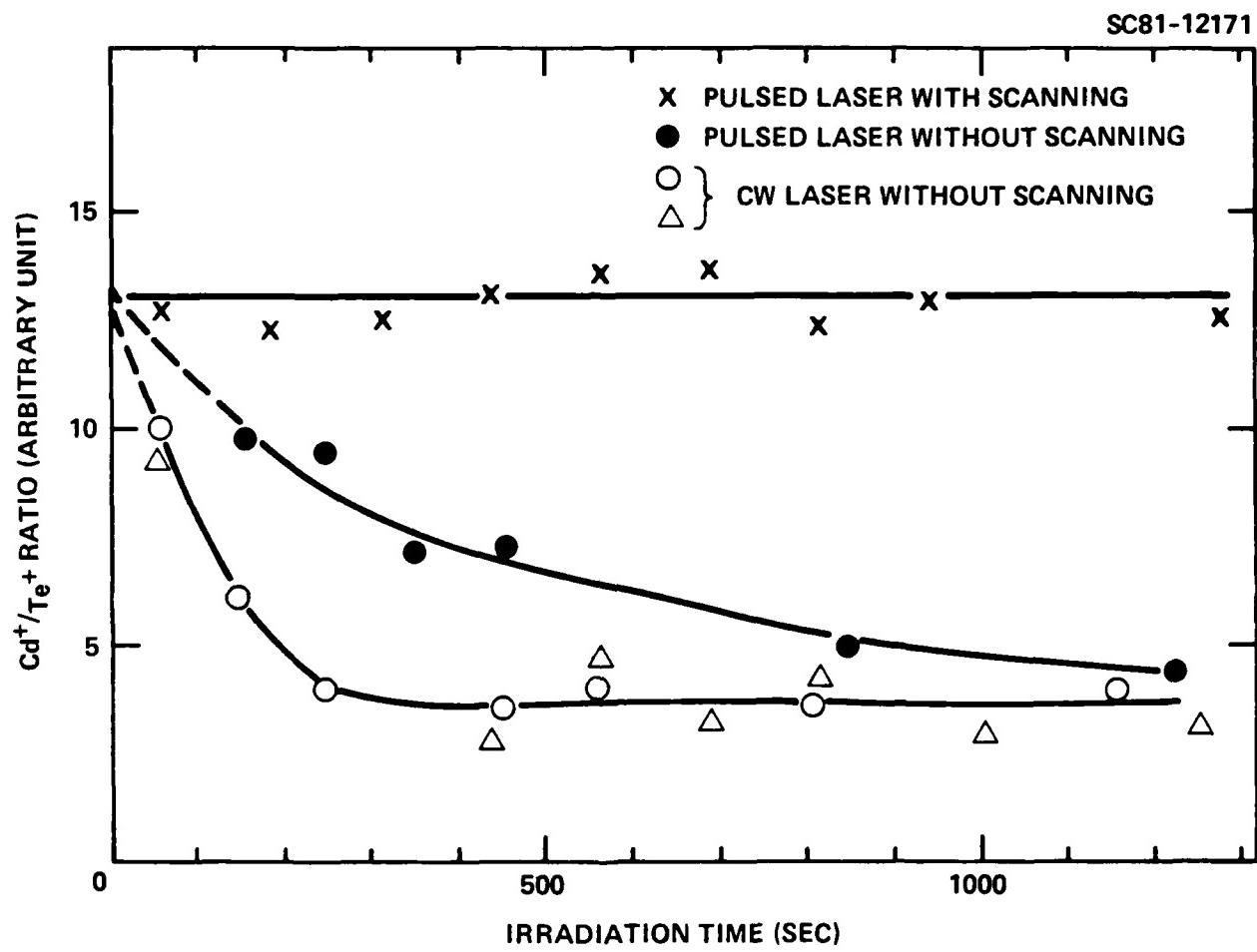


Fig. 14 Variation of Cd to Te from CdTe under various laser irradiating conditions.

compounds. 70 mole % of HgTe and 30 mole % of CdTe powders were mixed thoroughly and pressed into a pellet. A mass spectrum under the laser power density of 8×10^6 W/cm² and a pulse to pulse distance of 5×10^{-4} cm is shown in Fig. 15. The laser spot is large ($>100 \mu\text{m}$) in comparison with the size of the powder particles ($\sim 2-3 \mu\text{m}$); therefore, each pulse would sample enough material to be representative of the overall composition. As expected, the mass spectrum is just the superimposition of the two components. Only atomic Hg, Cd, Te, and a trace of Te₂ are present. The ratio of each evaporant species remains constant over a wide range of laser power density and scanning rate, and the constant ratio can also be maintained throughout the long duration of irradiation. These findings imply a congruent evaporation. The results are also reflected in the stoichiometric composition of the deposited film which is discussed later.

Because of differences in their optical and thermal properties, the evaporation rate dependence on the scanning rate of HgTe and CdTe are quite different. As shown in Figs. 10 and 13, the evaporation rate of HgTe has a greater dependence on the scanning rate than does that of CdTe. In a homogenized mixture, if the evaporation of the two compounds are independent of each other, the composition of the evaporants can be vary over the scanning rate. If this occurs, it will be difficult to obtain a stable and stoichiometric evaporation from a HgTe/CdTe mixture by using a pulsed laser.

We measured the evaporation rate of Hg and Cd from the mixture as a function of the scanning rate; the results are shown in Fig. 16. Both elements showed a decrease in intensity with an increase in the scanning

SC5202.11FR

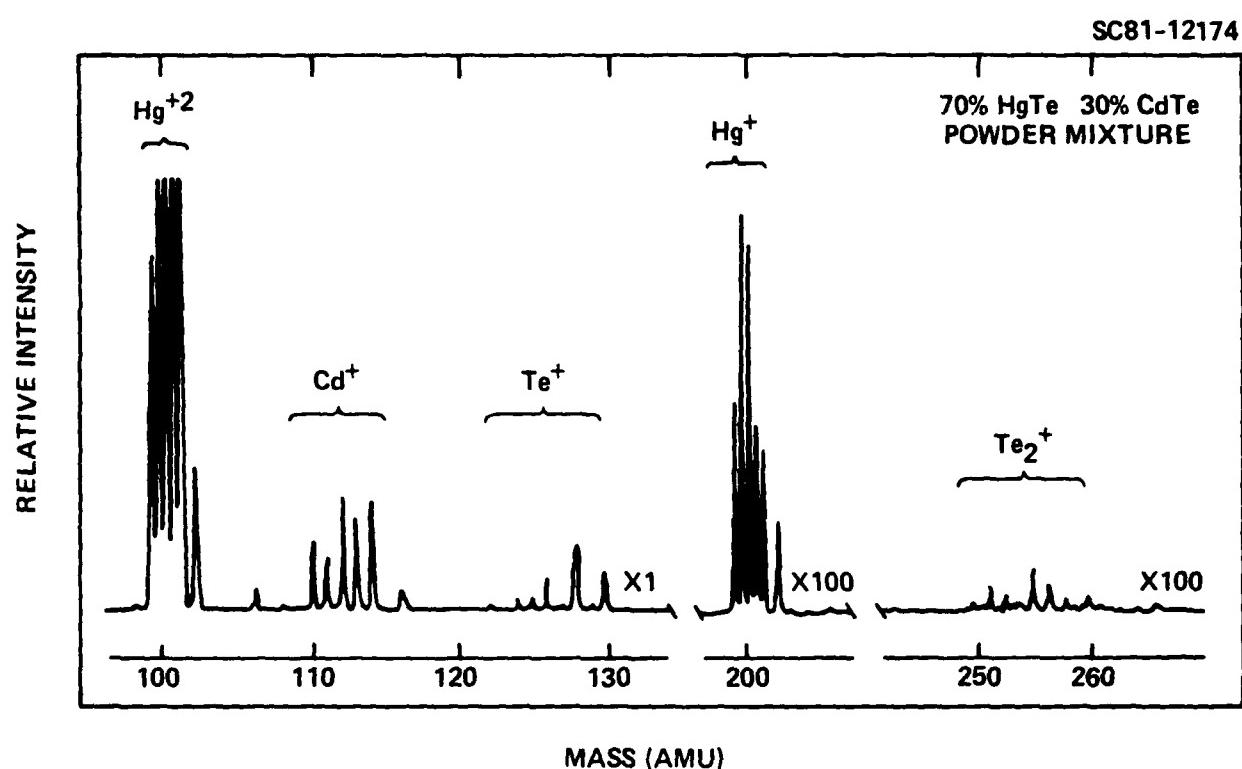


Fig. 15 Mass spectrum of laser evaporate HgTe/CdTe mixture.

SC5202.11FR

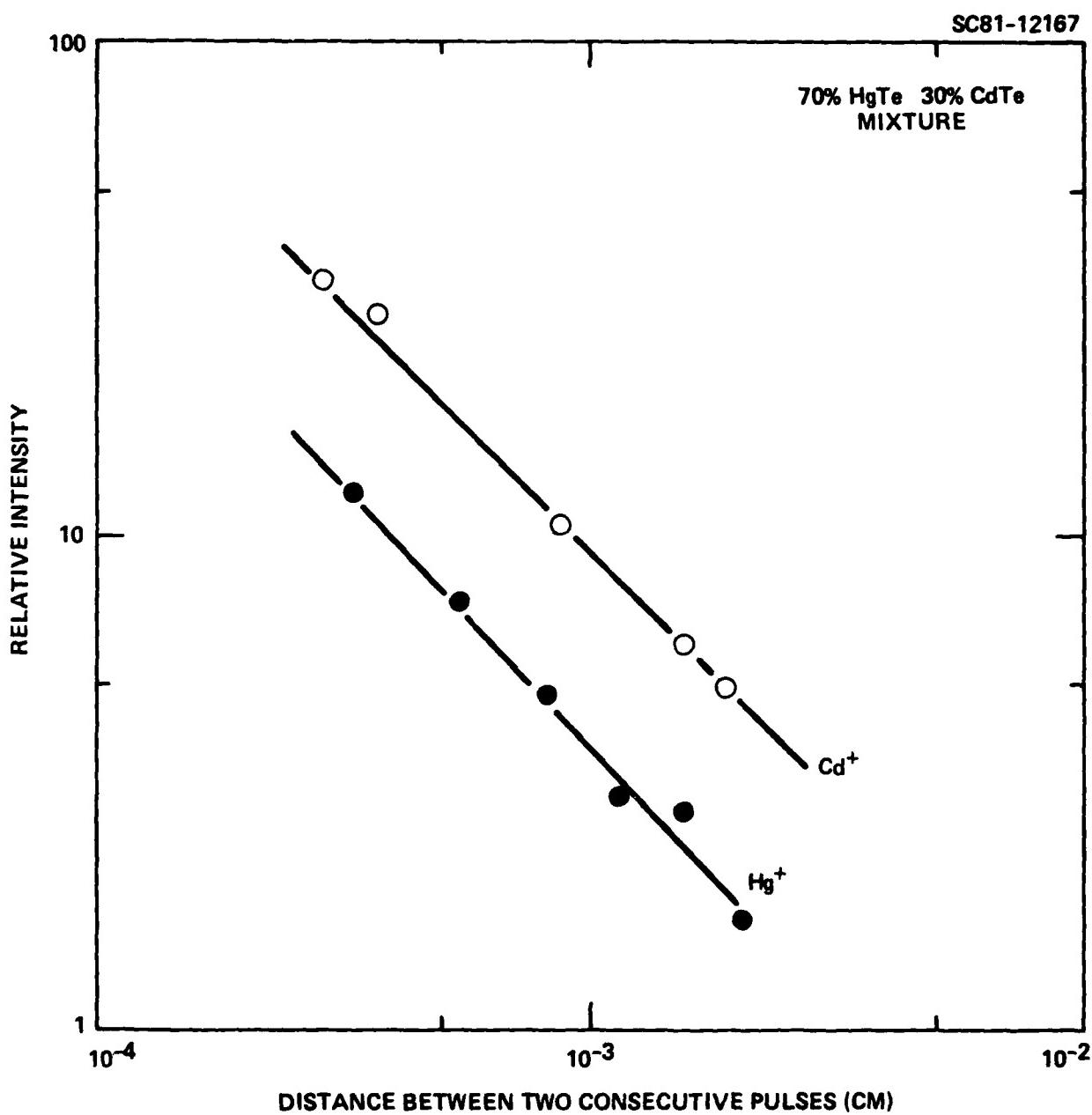


Fig. 16 Evaporate rate of Hg and Cd from a HgTe/CdTe mixture as a function of the scanning rate.

rate. The most important aspect, however, was that both decreased at the same rate, i.e., the ratio of Cd and Hg was constant over the entire range. This requires a thermal equilibrium between HgTe powders and CdTe powders in the mixture. A comparison of the dependence of evaporation rate on the scanning of three material systems in Fig. 10, Fig. 13 and Fig. 16 provides some clues to the laser absorption and heat transfer mechanism. The evaporation rate dependence of the mixture on the scanning rate is similar to that of HgTe, but much stronger than that of CdTe; this suggests that most of the laser radiation was first absorbed by the opaque HgTe. The thermal power was then transferred to CdTe powders until an equilibrium was reached.

3.2.3.4 Evaporation Bulk $Hg_{0.7}Cd_{0.3}Te$

We have also measured the mass spectrum by laser evaporating a piece of bulk $Hg_{0.7}Cd_{0.3}Te$ material under same conditions described in the previous section. The mass spectrum, shown in Fig. 17, is similar to that for the homogenized mixture. This suggests that the powder mixture can indeed substitute for the bulk material as an evaporation source.

3.3 Deposition Mechanism and Film Properties

The deposition mechanisms of laser evaporation and thermal evaporation are quite different because of the differences of their evaporants. These differences are:

SC5202.11FR

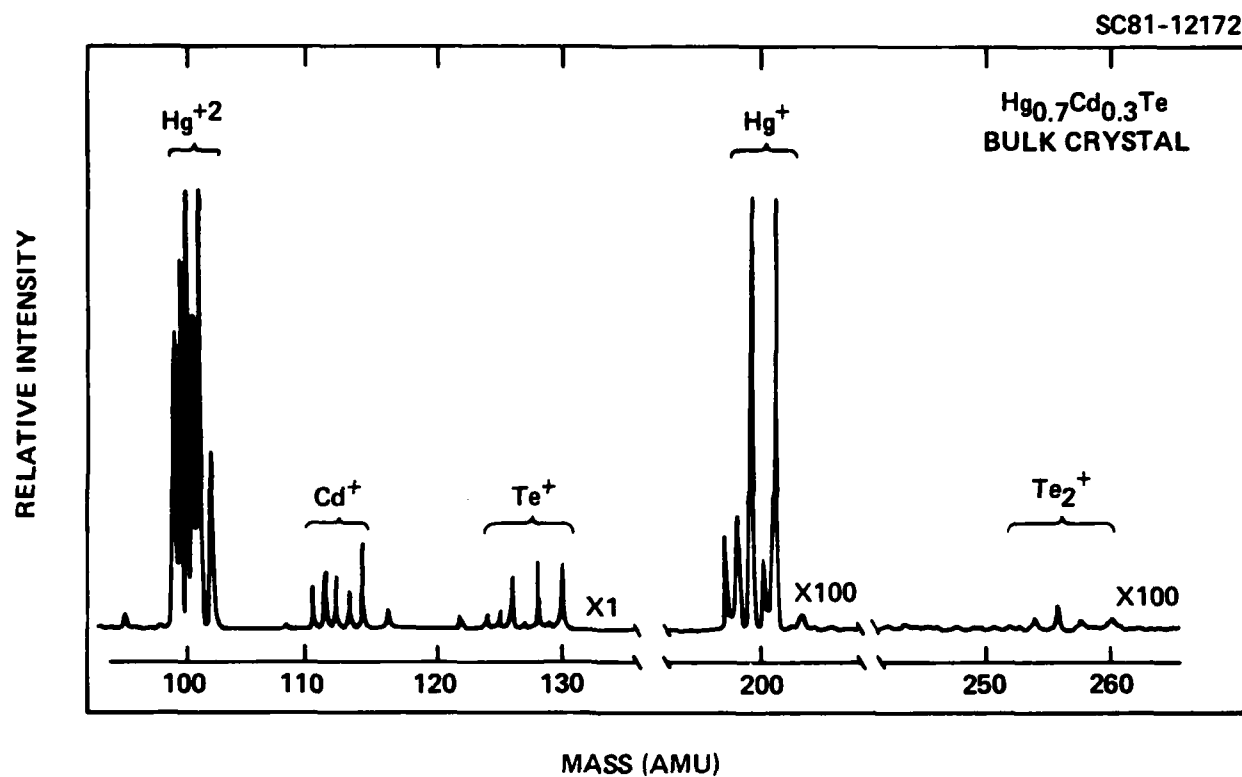


Fig. 17 Mass spectrum of laser evaporated bulk $\text{Hg}_{0.7}\text{Cd}_{0.3}\text{Te}$ material.

1. Laser evaporated species have high kinetic energy, typically of a few eV. The kinetic energy of thermal evaporated species, however, is small, only on the order of kT , where T is the source temperature.
2. The nature of the laser evaporated species is dependent on the laser power density. These species can have various forms, from microparticles to molecular clusters to atoms. However, thermal evaporation of a II-VI compound always produces atoms of the group II elements (e.g., Hg, Cd) and molecules of the group VI elements (e.g., Te₂).

Their effect on the deposition mechanism and film property are discussed in the following sections.

3.3.1 High Laser Power

When a piece of bulk Hg_{0.7}Cd_{0.3}Te material was irradiated with high power pulses, the surface erupted into small micron size particles. Some of the particles were solid chunks and others were the condensation from molten droplets. The surface of a film deposited under this condition is shown in Fig. 4. The laser parameters should be adjusted to stay away from this condition.

3.3.2 Intermediate Power Level

As described in Section 3.2.2, under intermediate power level, $Hg_{0.8}Cd_{0.2}Te$ evaporates mainly as molecular clusters, with a small amount of each constituent element in their atomic form. The kinetic energy of the evaporants is very high, perhaps as much as a few eV, as suggested by the time-of-flight measurement on Hg.

3.3.2.1 Film Properties

Films about 1.5 μm thick were deposited on <111> CdTe under intermediate power level conditions at room temperature. The base pressure of the vacuum was 5×10^{-7} torr. The substrate was placed at 40° from the incident laser beam to reduce the splashing. Nominal deposition rate was about 0.6 $\mu m/h$.

The surface of the film was smooth and had no discernable crystalline feature. EDAX study of its composition indicates Hg deficiency. In comparison to the composition of the target source, about 5% of Hg was lost during the evaporation-deposition process.

Optical transmission spectra of the thin film were taken at different locations, as shown in Fig. 18. The three curves are very close, indicating good compositional uniformity. Hg deficiency is also reflected in the absorption edge, which is at a shorter wavelength than a stoichiometric $Hg_{0.8}Cd_{0.2}Te$ material should be. Film composition also depends on the laser power. By increasing the power densities from 2×10^7 W/cm² to 7×10^7 W/cm² while

SC5202.11FR

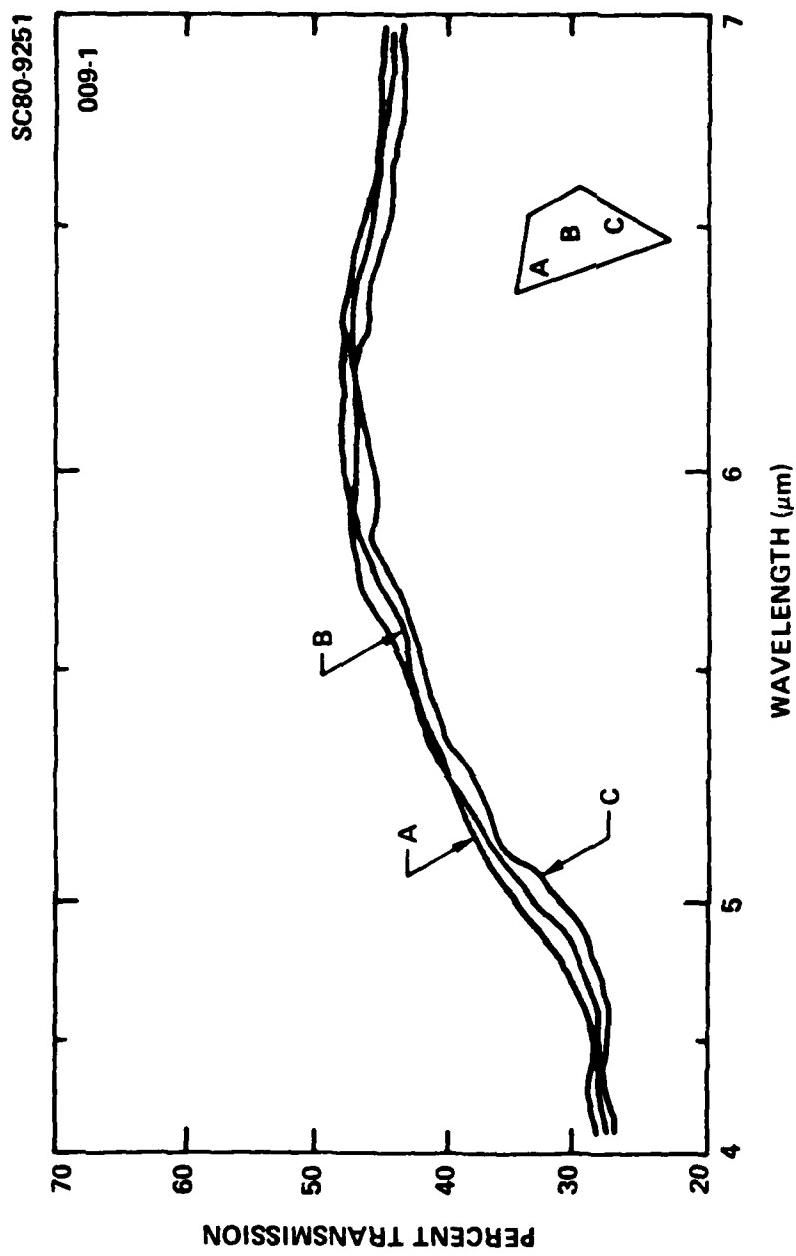


Fig. 18 IR transmission spectrum of a HgCdTe film.

keeping the scanning rate constant, films with absorption edges from 5.2 μm (74% Hg) to 3.0 μm (59% Hg) can be obtained, respectively.

The films are photoconductive. A photoconductor was made. The spectral response at 77K is shown in Fig. 19. Hall measurements were carried out to characterize the electrical properties. At 300K, the film is n-type with a carrier concentration of $7 \times 10^{16} \text{ cm}^{-3}$ and a mobility of 200 V cm^{-1} . At 77K, the film remains n-type with a carrier concentration of $2 \times 10^{16} \text{ cm}^{-3}$ and a mobility of 310 V cm^{-1} .

3.3.2.2 Deposition Mechanism

The deposition mechanism proposed in the following is consistent with these observations: The beam produced by radiation at this power level is a mixture of atoms and clusters, all of which possess a high kinetic energy of a few eV. In order for these species to stick onto the substrate surface on impingement, this large amount of kinetic energy has to be accommodated into the substrate in one collision. When a molecular cluster, consisting of N atoms, impinges the surface, the impact energy can be redistributed into its $(3N-6)$ vibrational modes to promote surface adhesions. But the sticking coefficients of the fast atoms will be much less than unity, because the excessive collision energy cannot be redistributed. One possibility of stabilizing them on the surface is by the formation of a metal telluride bond with a tellurium site on the surface. The bond energy of CdTe is stronger than that of HgTe; therefore, the sticking coefficient for Cd atom should be higher. Consequently, the deposited film is Hg deficient.

SC80-9587

SC5202.11FR

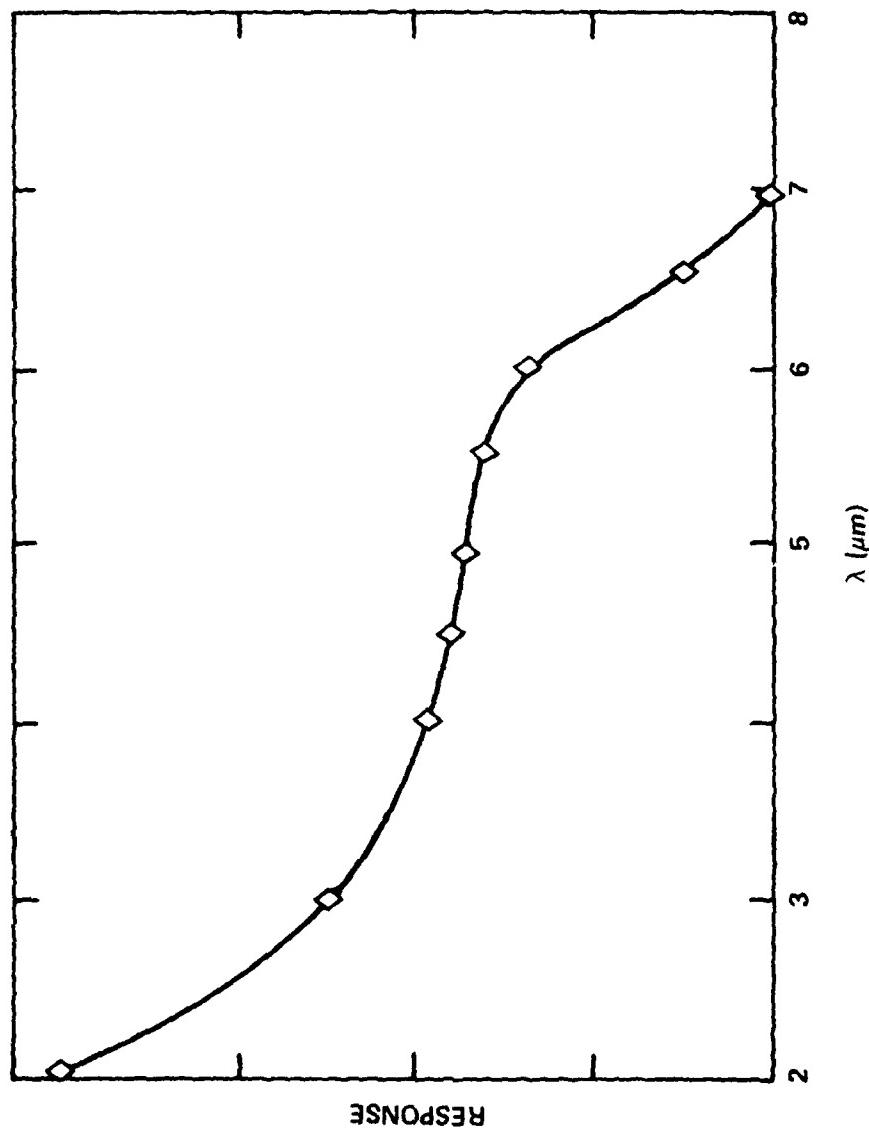


Fig. 19 Spectral response of a HgCdTe photodetector.

When the laser power is increased, the problem worsens in two ways. First, under high laser power and very slow scanning rate, there is an excessive amount of atomic mercury (i.e., less Hg in the clusters). Second, the kinetic energy of the atoms increases and thus decreases the sticking coefficient. The combination of these two effects can result in films with more Hg deficiency.

3.3.3 Low Power Level

At low laser power level, all the materials studied in this experiment vaporized mainly as atoms; their kinetic energies were lower. The laser pulse frequency can be increased to achieve the same beam flux, so that the deposition rate is not affected. At this power level, the signal of the mass spectrometer after each pulse is too weak for time-of-flight measurement. However, by assuming proportionality between the laser power and the evaporants' kinetic energy, we can estimate the kinetic energy of these atoms to be about 1 eV. This energy is comparable to the bond energy of HgTe, but is less than the bond energy of CdTe.¹⁰

3.3.3.1 Deposition of $Hg_xCd_{1-x}Te$ Film

$Hg_{1-x}Cd_xTe$ films have been obtained by evaporating both $Hg_{1-x}Cd_xTe$ bulk material as well as the powder mixture of the two compounds $(HgTe)_{1-x}/(CdTe)_x$; under the same conditions, similar films could be obtained. The results suggest that the powder mixture of HgTe and CdTe can be used effectively as a target source, which offers two advantages: first, it

is easily available, and second, the composition can be adjusted. The powder mixture was used in all the experiments described in this section. Films deposited in high vacuum and in a Hg background showed different properties; results are discussed in the following.

Deposition in High Vacuum

Powder mixture of HgTe (70%)/Cd (30%) was evaporated by low power laser pulses in a vacuum of 5×10^{-7} torr. The film deposited on CdTe substrate at room temperature showed deficiency in mercury both by EDAX and IR transmission measurements. Between 8 and 10% of Hg was lost.

Since we have indicated in Section 3.2.3.3 that the evaporation of (HgTe)/(CdTe) mixture under this condition is congruent, the mercury deficiency must occur in the deposition process. A plausible explanation for this again involves the high kinetic energy of the evaporants. The impact energies of these atoms are comparable to the bond energies of CdTe and HgTe. Since the HgTe bond is weaker, the probability of sticking a Hg atom on the substrate by reacting with tellurium to form HgTe is less than that for Cd. Overall, this leads to the formation of a Hg deficiency film.

Two previous experiments, which were carried out under completely different conditions, support this argument. Kraus et al⁵ sputtered $Hg_{1-x}Cd_xTe$ in an Ar plasma; the film deposited at room temperature was Hg deficient. In this case, the atomic species generated by sputtering processed high kinetic energy, much like our experiment; therefore, Hg deficiency was

probably due to the same cause. In another experiment, Hohnke et al⁴ used flash evaporation to deposit $Hg_{1-x}Cd_xTe$ film on a substrate at room temperature; the film was stoichiometric. In this case, the source was vaporized thermally. The kinetic energy of the evaporants was low and played no role in affecting the sticking coefficient.

Deposition in Hg Atmosphere

Since the Hg deficiency is caused by the high impact energy of Hg atoms on the substrate surface, one way to compensate for this is to provide a flux of low energy Hg atoms onto the surface during deposition. The simplest approach is to carry out the deposition in the vacuum chamber with a back pressure of Hg during the deposition. In our vacuum, we installed a pool of Hg to obtain this needed back pressure. By varying the opening of the gate valve to the pump, the background pressure of Hg could be varied from 2×10^{-5} torr to 10^{-3} torr.

In experiments where the substrate is at room temperature, only 2×10^{-5} torr of Hg background pressure is sufficient. Under this pressure, the flux of the Hg atom on the substrate surface is approximately 6×10^{15} atoms/s cm^2 , which is higher than the flux of Hg in laser evaporated beam. Also, at this pressure, the mean free path for collision is too long ($\sim 10^2$ cm) for any gaseous interaction to be important. Therefore, any effect on film composition can only be traced to gas - surface interaction. Figure 20 shows IR transmission spectra of two HgCdTe films deposited from laser evaporating from the same target source but under different vacuum condition. The film

SC5202.11FR

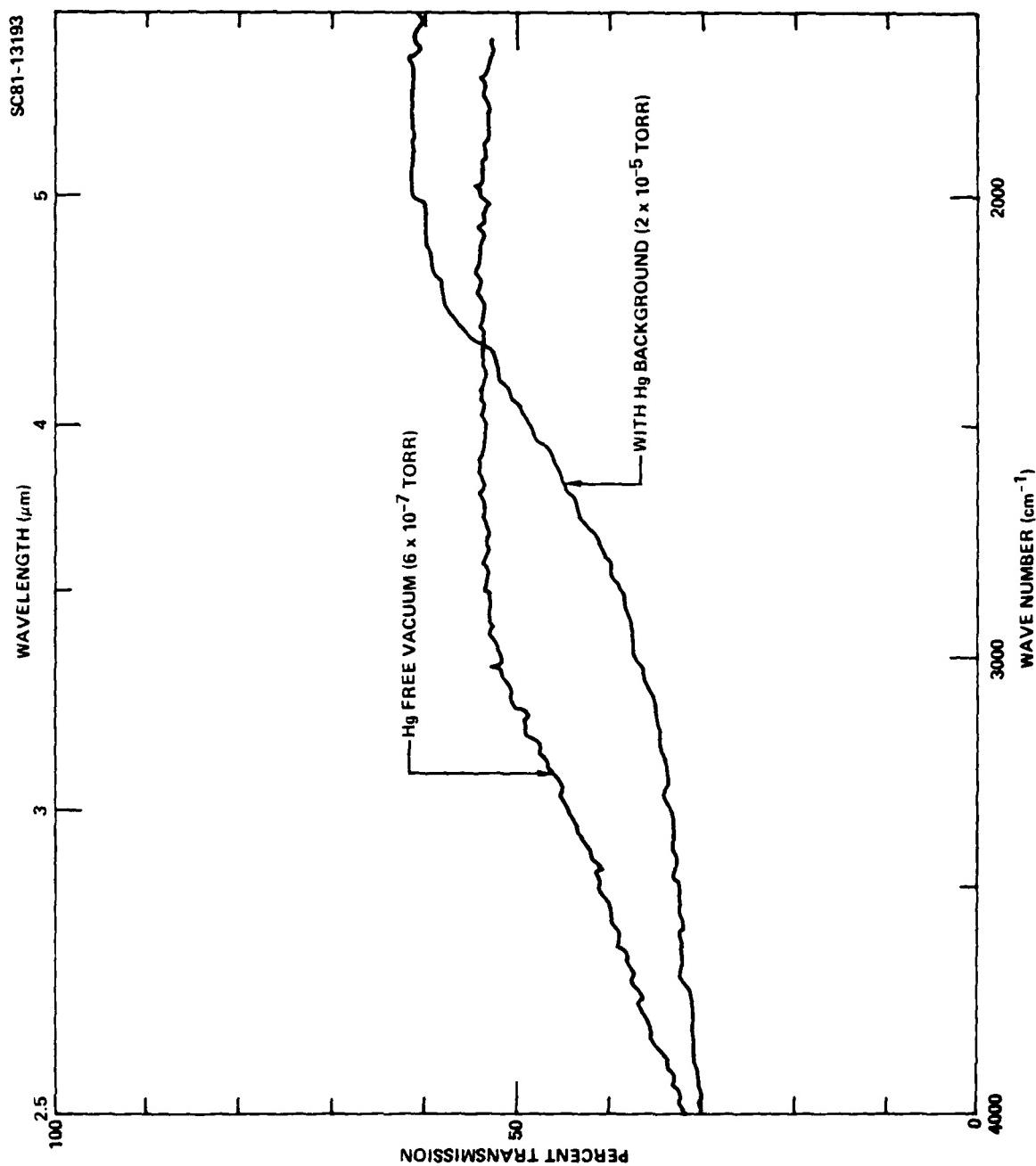


Fig. 20 IR transmission spectra of HgCdTe films deposited under different vacuum conditions.

deposited in 2×10^{-5} torr of Hg back pressure is stoichiometric and has an absorption edge near $4 \mu\text{m}$; however, for the film deposited in a Hg-free vacuum, the absorption edge is at a much shorter wavelength.

Film Properties

Thin films were deposited on CdTe from a HgTe (70%)/CdTe (30%) source at room temperature; a Hg back pressure of 3×10^{-5} torr was used during deposition. These films generally have mirror-like surface, and smooth interface with substrate, although there is still a very small amount of splashing. The surface morphology and a cross sectional view are shown in Fig. 21a,b.

One $\text{Hg}_{0.7}\text{Cd}_{0.3}\text{Te}$ film, 3700 Å thick and deposited on <111a> substrate under same conditions, it was sent to Prof. T. Sigmond of Stanford University for Rutherford ion backscattering analysis. The channeling spectrum of He^{+2} particles is shown in Fig. 22. The leading edges due to the backscattering from Hg, Cd, and Te atoms are resolvable. The scattering yield from the film is much higher than that from the bulk, indicating the film is amorphous.

Measurements of the electrical properties, obtained by Hall measurements at 300K and 77K, showed that the layers were all n-type, with carrier concentrations in the range of 5×10^{16} to $8.5 \times 10^{16} \text{ cm}^{-3}$ at 300K and 3.7×10^{16} to $7 \times 10^{16} \text{ cm}^{-3}$ at 77K. The mobility is quite low, typically around $150 \text{ cm}^2/\text{Vsec}$. These values are in good agreement with the measurements on the room temperature deposited $\text{Hg}_{0.7}\text{Cd}_{0.3}\text{Te}$ film made either by flash evaporation⁴ or sputtering⁷ in a Hg atmosphere.

SC5202.11FR

SC81-13234

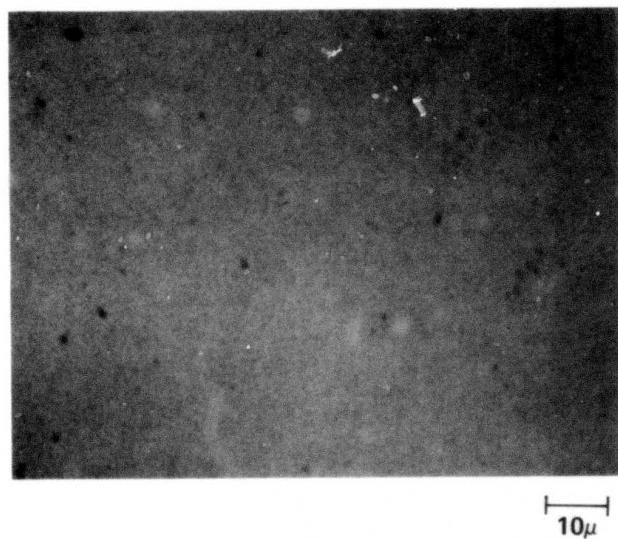


Fig. 21(a) Surface of a HgCdTe film.

SC5202.11FR

10 μm

SC80-11263



Fig. 21(b) Cross section view of a HgCdTe film.

SC5202.11FR

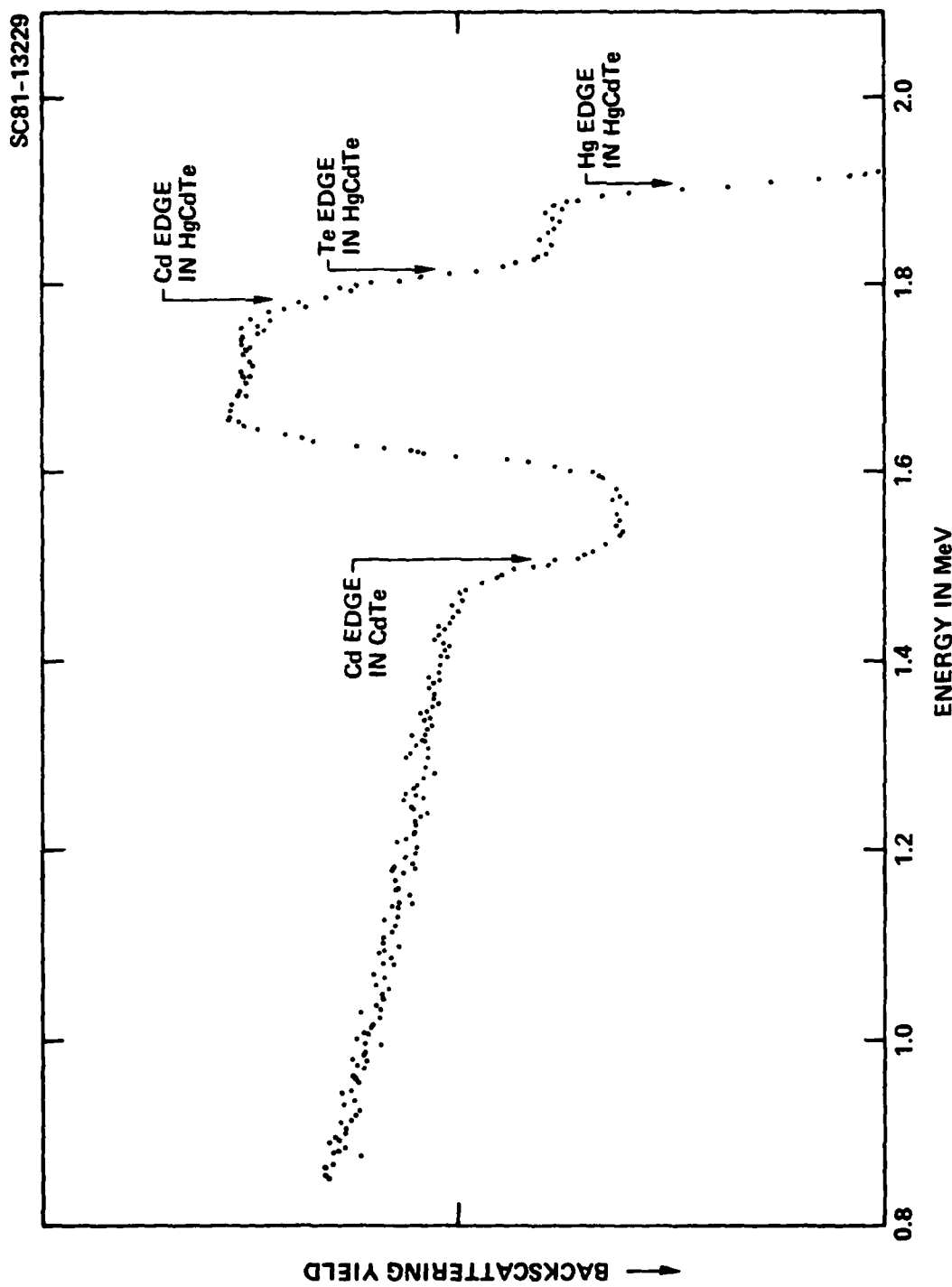


Fig. 22 Rutherford backscattering of 3700 Å $\text{Hg}_{0.7}\text{Cd}_{0.3}\text{Te}$ on CdTe.

In one experiment, the substrate was heated to 170°C during the deposition of a $\text{Hg}_{0.7}\text{Cd}_{0.3}\text{Te}$ film; the surface of the film is shown in Fig. 23. In this section of the substrate, there are two crystal grains: one has a <111> orientation; the orientation of the other grain is about 15° off. On the <111> oriented area, the film has a very fine grain structure. On the unoriented area, the film appears to be much rougher. The morphological dependence on the substrate orientation is an indication that on a 170°C substrate, there is some oriented growth in film formation rather than just an "overcoating." The electrical properties of this film, which, is n-type, are much better than those deposited at room temperature. The carrier concentration is $8 \times 10^{16} \text{ cm}^{-3}$ at 300K, and $6.7 \times 10^{16} \text{ cm}^{-3}$ at 77K. The mobility is $2 \times 10^3 \text{ cm}^2 \text{ V}^{-1} \text{ s}^{-1}$ at 300K and $2.4 \times 10^3 \text{ cm}^2 \text{ V}^{-1} \text{ s}^{-1}$ at 77K.

In order to improve the crystallinity, and thus its electrical properties, two other approaches were also tried:

1. The as-deposited films were sealed in a quartz tube containing Hg and were thermally annealed for 8 hours at 250°C. Although the films recrystallized in the <111> direction, as shown in Fig. 24, their sizes were too small.
2. Both in situ and post laser annealing were briefly tried. In some cases, the structureless as-deposited film showed some ordered orientation after laser irradiation, suggesting some crystal regrowth. However, because of its added complexity to a

SC5202.11FR

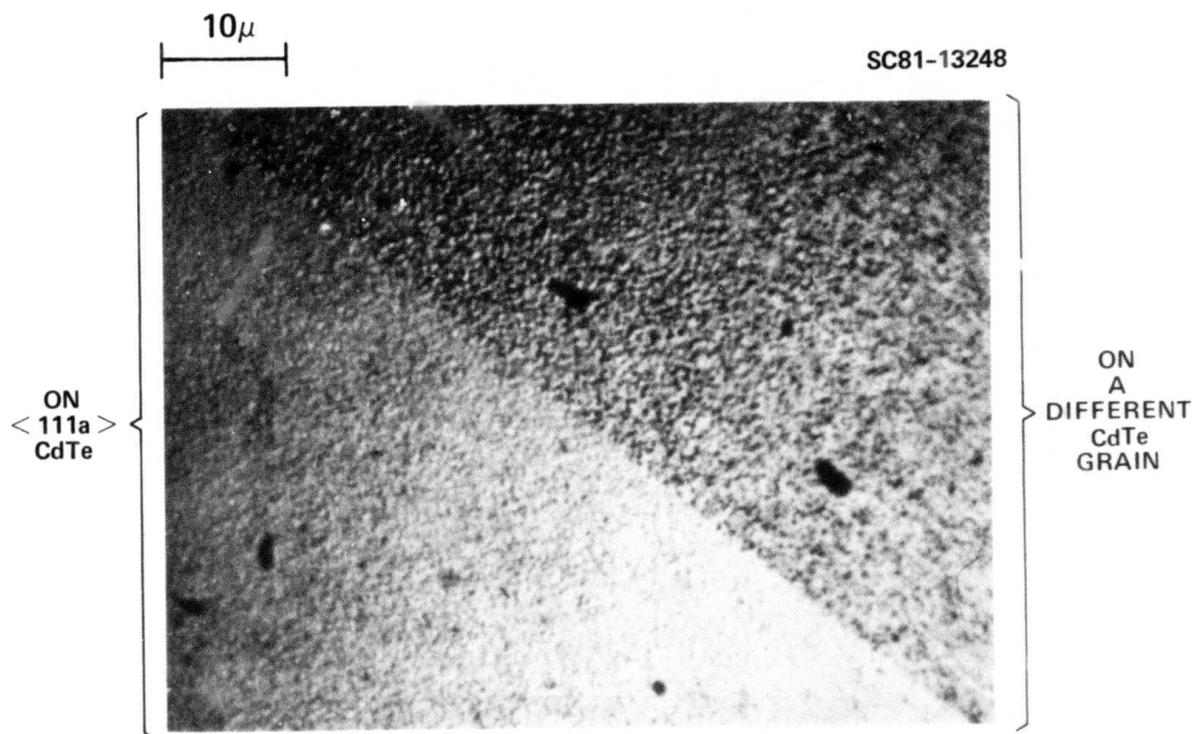


Fig. 23 Surface of a HgCdTe film deposited at 170°C.

SC5202.11FR

SC81-12529

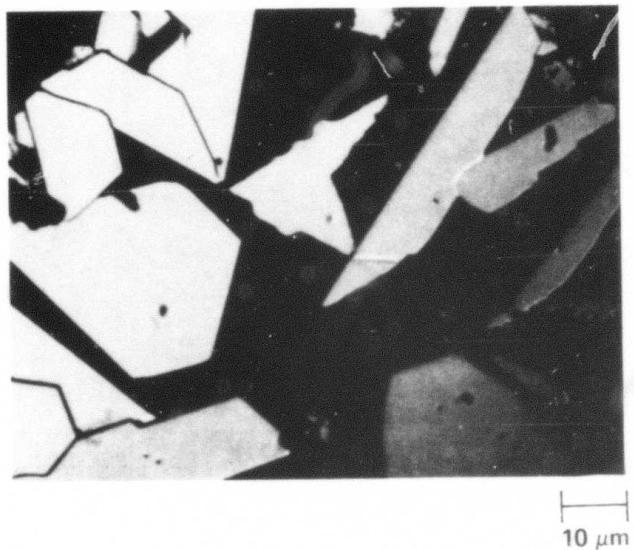


Fig. 24 $\text{Hg}_{0.7}\text{Cd}_{0.3}\text{Te}$ film on CdTe after thermal treatment.

SC5202.11FR

still developing new technique, we decided to postpone any in-depth study of this subject. Meanwhile, post laser annealing and Rutherford backscattering for characterization work will be carried out by prof. T. Sigmond and J. Gibbons at Stanford University in a collaborative effort.

4.0 CONCLUSION

Our new technique for depositing thin HgCdTe films uses pulsed irradiation from a high power laser to evaporate source material and to anneal the deposited film. We have laid down a considerable amount of ground work in perfecting this technique. Thus far, most of our efforts have been concentrated on understanding and controlling the laser evaporation-deposition process.

Since the condition of laser evaporation is different from other conventional thin film techniques, a thorough understanding of the evaporation/deposition mechanism seems to be necessary for process optimization. In this study, we have used mass spectroscopic analysis to elucidate the mechanism for four materials: HgTe, CdTe, HgTe/CdTe mixture, and $Hg_{1-x}Cd_xTe$ bulk material. Some of the key results are:

1. Evaporation depends strongly on laser power density level and scanning rate.
 - A. Under a very high laser power level, most of the $Hg_{0.7}Cd_{0.3}Te$ material "splashed" into the vacuum as micron size particles.
 - B. Under intermediate laser power level, splashing of $Hg_{0.7}Cd_{0.3}Te$ occurred to a lesser extent. A large number

of molecular clusters and some atomic species were also produced.

C. Under low laser power level:

- (1) All four materials evaporate exclusively as atomic species (Hg, Cd, and Te) and a trace of molecular tellurium.
- (2) Evaporation rates decrease with the increase of scanning rate; this is related to the thermal property of the material.
- (3) Evaporation is stoichiometric over a wide range of power level and scanning rate.
- (4) Under pulsed irradiation with extremely slow scanning rate, or under cw irradiation, preferential evaporation of Hg and Cd from HgTe and CdTe, respectively, can occur. Depletion of Hg occurs at lower temperature, whereas a surface temperature as high as 1700°C is required for depletion of Cd from CdTe.

- (5) HgTe (70%)/CdTe (30%) mixture yields the same evaporants as $Hg_{0.7}Cd_{0.3}Te$ under pulsed irradiation. In the case of the mixture, most of the irradiation energy was first absorbed by the opaque HgTe and then transferred to CdTe until a thermal equilibrium is established.
2. Deposition of HgCdTe depends on the vacuum condition. In a Hg free vacuum, the deposited film is mercury deficient. In a vacuum with some Hg back pressure, the deposited film becomes stoichiometric.

Using the knowledge obtained from these mechanistic studies, we have performed some preliminary experiments and demonstrated that stoichiometric $Hg_{1-x}Cd_xTe$ film of various compositions ($x = 0.3$ and 0.25) can be obtained by laser evaporating HgTe/CdTe mixture of the corresponding compositional ratio. Besides HgCdTe, this new technique also appears to be suitable for depositing thin films of other volatile materials which do not evaporate congruently by other thermal means.

5.0 FUTURE PLAN

Future emphasis will be on process optimization and device fabrication. More specifically, some of our future plans are:

1. Hardware Improvement: Although the LADA apparatus has been debugged quite extensively, there are still some areas for improvements. For example, a heater will be installed on the target source holder; this will be used to thoroughly outgas the powder pellets prior to deposition in order to minimize splashing.

Another area for improvement involves the mirror assembly that reflects the incoming laser beam onto the target source for evaporation. The use of this mirror avoids the "window clouding" problem which blocks the laser beam. However, even with the mirror, deposits can still accumulate on the mirror surface, causing gradual deterioration in the mirror's reflectivity and a reduction of the evaporation rate. The mirror therefore has to be removed periodically from the vacuum chamber for cleaning. We will use a metallic mirror (such as molybdenum mirror) and mount it to a heater. During deposition, the mirror will be heated to an elevated temperature to completely prevent any condensation. This way, a constant evaporation rate can be achieved, and the mirror maintenance will be a minimal.

There are also many other apparatus improvements. Our goal is to make the LADA apparatus a routinely operational machine, just like the already developed sputtering E-beam and many other thin film techniques.

2. Laser Beam Processing: Laser processing will be carried out in more detail. The major emphasis will be the use of a laser beam scanned over the substrate prior to deposition for surface cleaning. The laser beam will also be scanned over the substrate during deposition in order to remove any micro-particles splashed onto the film. Since the bonding of these particles to the film surface is weaker than the bonding of the atoms in the film, it is possible to use a laser beam to remove such particles without interacting too strongly with the film.

Collaboration with Prof. J. Gibbons and T. Sigmond on laser annealing will be continued.

3. $Hg_{1-x}Cd_xTe$ films more than 5 μm thick with both $x = 0.3$ and $x = 0.2$ compositions will be deposited on CdTe and other foreign substrates (Si, sapphire, and InSb). The films will be characterized and fabricated into photoconductive or photovoltaic devices. Post thermal annealing in Hg environment in order to improve its electrical properties will also be investigated.

4. In addition to the HgCdTe system, we will venture into other materials such as ZnO. A new chamber has already been designed and is under construction for this purpose.

6.0 REFERENCES

1. R.F.C. Farrow, G.R. Jones, G.M. Williams, P.W. Sullivan, W.J.O. Boyle and J.T.M. Wetherspoon, *J. Phys. D*, 12, L117 (1979).
2. R. Ludeke and W. Paul, *J. Appl. Phys.* 37, 3499 (1966).
3. S.A. Ignatowicz, A. Kiseil and M. Zimnal, *Thin Solid Films*, 21, 231 (1974).
4. D.K. Hohneke, H. Holloway, E.M. Logothetis and R.C. Crawley, *J. Appl. Phys.* 42, 2487 (1971).
5. H. Kraus, S.G. Parker and J.P. Smith, *J. Electrochem. Soc.* 114, 616 (1967).
6. A. Zozime, C. Sella and G. Cohen Solal, *Thin Solid Films*, 13, 373 (1972).
7. R.H. Cornely, L. Suchow, T. Gabara and P. Diodato, *IEEE Trans. Elec. Dev.* ED-27, 29 (1980).
8. J.F. Ready, *Appl. Phys. Lett.* 3, 11 (1963).
9. J.F. Friichnicht, *Rev. Sci. Instrum.* 45, 51 (1974).
10. P. Goldfinger and M. Jeunehomme, *Trans. Far. Soc.* 59, 2851 (1963).

DISTRIBUTION

Director
Defense Advanced Research Projects Agency
1400 Wilson Blvd.
Arlington, VA 22202

Attn: Program Management (2)
Attn: Sven Roosild (1)

Defense Documentation Center (12)
Cameron Station
Alexandria, VA 22314

Director (1)
Night Vision & Electro-Optics Laboratory
NVEOL-RD, Ft. Belvoir, VA 22060

Attn: Mr. William Guterrez

Science Center Distribution:

J. T. Longo	(1)
D. T. Cheung	(1)
Group Secretary	(2)
Contracts & Pricing	(1)
Library	Original + (1)
J. T. Cheung	(1)